THE HONG KONG POLYTECHNIC UNIVERSITY

Department of Electrical Engineering

FUZZY LOGIC CONTROL IN LINEAR SWITCHED RELUCTANCE MOTORS

by

Antares San-Chin Kwok

A thesis submitted

in partial fulfillment of the requirements

for the Degree of Master of Philosophy

September 2007

CERTIFICATE OF ORIGINITY

I hereby declare that this thesis is my own work and that, to the best of my knowledge and belief, it reproduces no material previously published or written, nor material that has been accepted for the award of any other degree or diploma, except where due acknowledgement has been made in the text.

_____ (Signed)

Antares San-Chin Kwok (Name of student)

Abstract

During the last decade, the Linear Switched Reluctance Motor (LSRM) has become popular in motor industry due to its structural simplicity, robustness, high power density, low cost and applicability in high temperature environment. However, its significant torque ripple from the flux nonlinearity creates difficulty on precision motion control.

This research project aims to develop a fuzzy logic control system to provide a high performance on LSRM based on switched reluctance actuator technology. The controller is designed to replace the conventionally used numerical approach on handling model nonlinearity problem.

For the preparation of high speed motion tests, the rigidity of the LSRM prototype is improved with advance mechanical features and special assembly procedures. This practice is promoted in industry to enhance the motor productivity.

The LSRM prototype is firstly investigated to study its force and current relationship. To shorten the real time computation time and simplify the control plant, a table look-up fuzzification is developed. With the help of software, LSRM motion tests are simulated before real experiment. The significant improvement on position

control strongly proves the success of the proposal. After that, the experimental result applying on the real prototype closely matches the simulation result.

In order to enhance the LSRM robustness and the position tracking responses, another fuzzy logic controller is newly designed and implemented to supervise the traditional Proportional-Differential (PD) control parameters. Combining the experimental results on inner control loop with current force relationship and outer control loop on PD parameter supervision, the fuzzy logic improves motor performance at least 20%.

With the successful application of the fuzzy logic, the LSRM system in this project is very robust and capable to provide a high precision motion performance. Based on the features of magnet-free and flexibility under high temperature, LSRM is believed to become popular in precision machine industry with fuzzy logic controllers.

Acknowledgements

I would like to express my sincere appreciation to my project supervisor, Dr. Norbert Cheung. His motivation and encouragement have been invaluable for me throughout the whole research period. He has always been patient and supportive towards the completion of the thesis.

Moreover, I would like to thank Mr. Wai-Chuen GAN, my co-supervisor in ASM Assembly Automation Hong Kong Ltd (AAA). His guidance is greatly useful and beneficial. Also, I would like to take the opportunity to thank Mr. Pei-Wei TSAI for his technical advice.

Based on the Teaching Company Scheme (TCS), I would like to thank AAA for the support on this research project. I have to thank all my valuable friends and colleagues, who have helped me out at the times of need. Their assistances are highly appreciated.

Finally, I would like to thank my family for their support during my research studies.

Table of Contents

List of Figures

List of Tables

List of Acronyms

CoA	Center-of-Area
DC	Direct Current
LHS	Left Hand Side
LM	Linear Motion
LSRM	Linear Switched Reluctance Motor
PC	Personal Computer
PD	Proportional-Differential
PID	Proportional-Integral-Differential
PWM	Pulse Width Modulation
RHS	Right Hand Side
RSRM	Rotary Switched Reluctance Motor
SRM	Switched Reluctance Motor

List of Symbols

$v(t)$	Phase voltage, V
$i(t)$	Phase current, A
$R(t)$	Phase resistance, Ω
t	Time, s
λ	Phase flux linkage, Vs
x	Travel distance, mm
f_e	Generated electromechanical force, N
f_l	External load force, N
M	Mass, kg
b	Frictional constant, kg/ms^{-1}
K_m	Average motor force constant, N/A
K_P	Proportional gain
K_D	Derivative gain
K_I	Integral gain
T_s	Settling time, s

Chapter 1

Introduction

In manufacturing industry, an electromagnetic motor is frequently applied for high-speed and precise robotic operations. One of the popular motors, Switched Reluctance Motor (SRM) is introduced with its background and principle.

Based on the nature of the motion, there are two main categories of SRM for rotary and linear operation. The characteristics of SRM are briefly presented to explain its popular industry applications.

From the view of motion control, the SRM nonlinearity characteristics still create much problems and it becomes the project motivation to provide the solution. Present literatures are discussed and an innovative controller is proposed to drive the SRM prototype. As a result, the achievements are summarized and the thesis organization is presented.

1.1 Overview

Due to the fast development of electronic and mechanical system recently, the robotic arm has become more important and frequently used in industry. Especially for semiconductor manufacturing, the fast and precise robotic motions are highly promoted to increase the machine productivity.

Beside the permanent magnet motor, SRM is one of the popular motors for robotic applications. A ‘reluctance’ motor is defined as an electric motor in which torque is produced by the tendency of its moveable part to move to a position where the inductance of the excited winding is maximized.

In general, SRM can be classified into two categories based on their operation principle. One of them is defined as rotary switched reluctance motor (RSRM) because it provides rotary motion as similar as typical stepping motor. The other group is linear switched reluctance motor (LSRM) which involves a translator as a linear motion actuator. Fig. 1.1 and Fig. 1.2 show the detailed structure of RSRM and LSRM respectively.

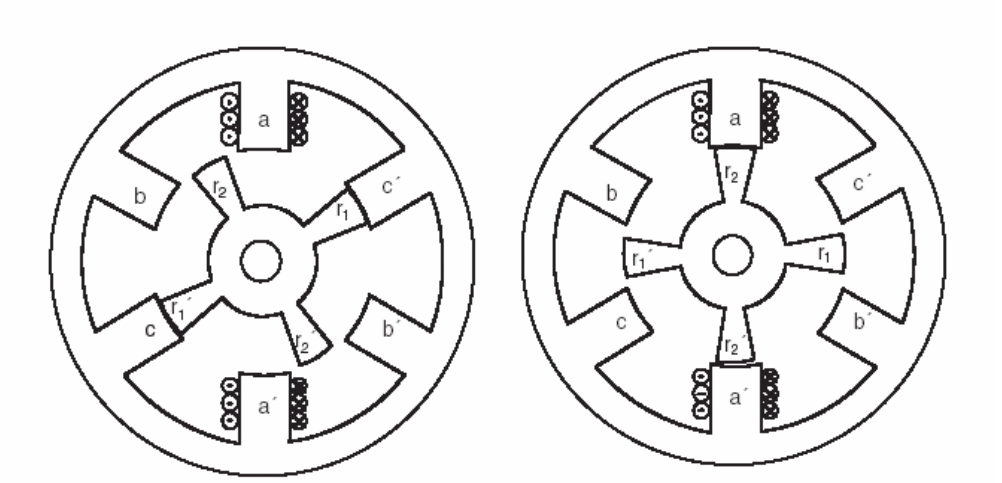

Fig. 1.1: Structure of RSRM where phase c or phase a aligned.

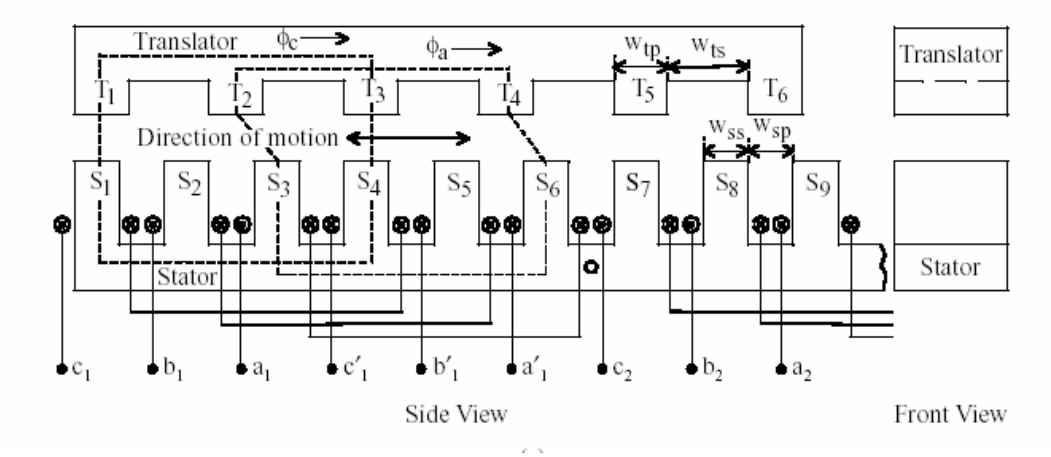

Fig. 1.2: Structure of LSRM with translator and stator.

1.2 LSRM characteristics

LSRM has become popular in motor industry during the last decade. Its usage is highlighted with its characteristics such as structural simplicity, robustness, high power density, low cost and promising flexibility in high temperature environment. In this section, the key advantages of the LSRM are summarized, leading to their facilitation in some applications.

I. The motor structure is simple and thus easy for maintenance. As shown in the Fig. 2, the motor only consists of windings and laminated steel plates with constant air gap between the translator and the stator. Such simple motor design can also improve LSRM robustness.

II. LSRM has a high power density to support high-speed operations. It is well known that the power density of stepping or servo motors drops at high velocity. On the other hand, LSRM can offer higher motor power than permanent magnet motor at high speed motion. LSRM is more suitable for high speed applications in semiconductor manufacturing.

III. The manufacturing cost and the material cost of LSRM are low. In LSRM, the coil windings are installed at the moving translator instead of fixed stator. In addition, the LSRM has no magnet and the laminated steel plates can be made by economical punching process. Consequently, the total fabrication investment is attractive when comparing with that for stepping or servo motor preparation.

IV. The SRM promises higher flexibility under different temperature environment. Due to the absent of magnets, the coil winding copper and the laminated steel plates in SRM have minimal temperature effects and keep their magnetic properties under high temperature.

V. LSRM provides direct drive motion with high precision. Linear motors are being increasingly applied in industry because of their simple mechanical designs. A LSRM is a flattened RSRM and can be used without gears, converters, belts and lead-screws for linear motions. Therefore, positioning accuracy is improved by the cancellation of gears' irregular teeth geometry and lead-screws backlash which contribute uncertainty in the linear motion.

Apart from the above advantages, LSRM still has the problem of torque ripple. Due to magnetic field nonlinearity in LSRM, the magnetic flux cannot be represented by linear functions along translator position or under different excitation currents. In order to solve the problem, literatures present different approaches and will be discussed in the next section.

1.3 Motivation

With the development of the power electronics and the research of various control algorithms, more recent literatures have been shown on reluctance motors application. However, seldom of them provide direct solution on the motion control of short distance and precise specifications. In [6], a few meters long prototype LSRM is designed from a RSRM. While the configuration consists of active stator and passive translator, windings cannot be used effectively and some coils are idol if the translator does not move over them. In [7], the application focuses on the torque control. Only the current control as well as the speed control is considered.

The motion control on LSRM is difficult due to its significant torque ripple resulting from friction uncertainty and flux nonlinearity. Base on reluctance motors characteristics and uneven air gaps, flux linkage cannot be represented as a linear function along the track. This excessive torque ripple causes undesired effect and make noisy on sliding and rotating assemblies.

Generally, compensation methods are applied by using a friction model to eliminate the nonlinear friction force. In [8], despite the model-base method can improve the performance, the control is not robust enough and depends on the parameter accuracy. At the same time, a complicated model analysis and mathematical equation are required for friction compensation.

This research aims to develop a fuzzy logic control system to provide a high performance on LSRM based on switched reluctance actuator technology in [1] and [2]. The fuzzy controller is designed to replace the conventionally used numerical approach on handling model nonlinearity problem. Consequently, much effort is saved to study the motor magnetic field characteristics and its mechanical rigidity.

In [9], [10] & [11], the fuzzy controllers are developed with simulations results without real experimental results. In this project, the proposed control algorithm would be evaluated by both simulation and experimental data.

In addition, a table look-up fuzzification is developed to shorten the real time computation time and simplify the control plant. Therefore, low grade CPU is sufficient to support the controller and the system cost is reduced.

Finally, in order to enhance the LSRM robustness and the position tracking responses, another fuzzy logic controller is newly designed and implemented to supervise the traditional PD control parameters. Typically, PD control gain need to be adjusted for different traveling distance to provide optimized performance. Applying fuzzy controller, these traditional control parameter can be well tuned automatically.

1.4 Summary of contributions

Through this project development, a LSRM prototype is prepared and fuzzy control algorithms are implemented with achievement.

I. One axis of LSRM prototype is completed. With improved coil winding mountings, the motor can have higher bandwidth and rigidity.

II. To do experiments on the LSRM, one set of drive hardware system is ready.

III. By using Matlab Simulink software, the offline motion simulation is done to check the proposed control algorithm.

IV. Based on the real LSRM prototype characteristics, the fuzzificed look-up table is development. The improvement in motion accuracy proves the success of the proposal.

V. With the help of PD fuzzy supervision, the LSRM is found to be more robust for different travelling distances.

1.5 Organization of the thesis

Chapter 1 introduces LSRM and lists out its characteristics. Fuzzy logic control approach is proposed to solve LSRM nonlinearity problems. The project motivations are stated and the contributions are summarized.

Three kinds of LSRM mechanism are compared in Chapter 2. The advantages and disadvantages are summarized to decide the finalized prototype motor for motion studies.

In Chapter 3, the detailed description of the LSRM prototype and the motor specifications are provided. At the same time, the operation principle is presented with pictorial explanation. In addition, the motion profiles for different traveling distances are plotted.

In Chapter 4, the fuzzy logic control is compared with the conventional numerical approach. The advantages of fuzzy logic are described with several successful applications. The table look-up fuzzification and control parameter supervising algorithm are introduced. The whole proposed controller is highlighted lastly.

Chapter 5 shows the experimental setup and the motor prototype. It also summarizes the project simulation and experimental results to evaluate the proposed controller.

Finally, the whole research project is concluded and the further research area is suggested in Chapter 6.

Chapter 2

Motor design comparisons

In this section, three types of planar LSRM prototypes are studied to compare their motor design features. Ignoring the control strategy applied, a simple mechanical structure with a high rigidity is appreciated for future precise and high-speed motion experiments. At the same time, manufacturing cost and fabrication time will be discussed to ensure high productivity.

2.1 Cassette type motor

Fig. 2.1 shows the first prototype, cassette type motor, where the total moving mass is about 10kg. The power supply has to provide a large amount of energy to drive the motor. In the simple prototype test, 10A current can only push the motor to move slowly. The power efficiency is very low.

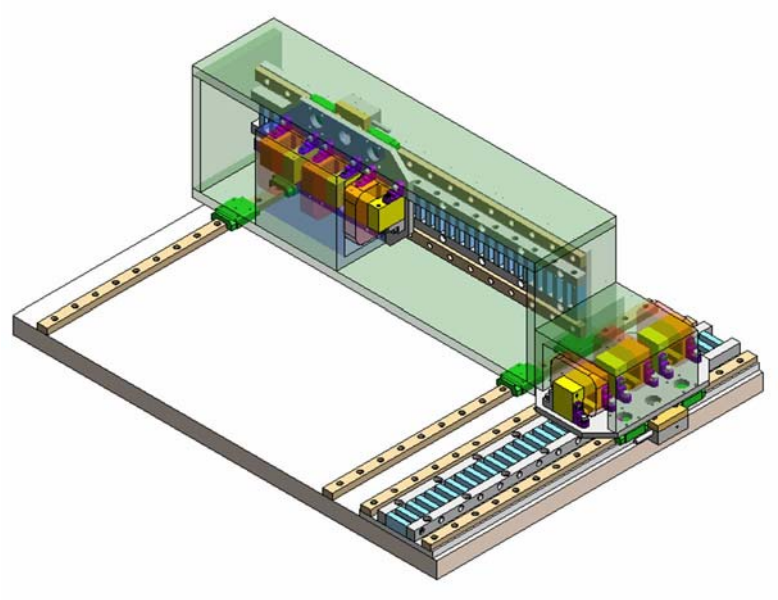

Fig. 2.1: Cassette type motor.

Due to the extremely heavy load, the profile time has to be multiple of that for other motors and is too long to fulfill robot pick arm motions requirement in semiconductor manufacturing. During motion tests, the average applied current is higher than 10A. The current is too high and creates safety issue problem. The coil wire should be altered to be thicker one for higher current to prevent explosion and thus the material cost increases. Therefore, the large moving mass and the high manufacturing cost become the cassette type motor significant disadvantages.

2.2 End supported type motor

The second design is named as end supported type motor and shown in Fig. 2.2. Its moving mass is much lower than the cassette type one. Shown in Fig. 2.3, the static laminated metal plate track is mounted above the moving platform. The magnetic attractive force between static and dynamic metal plate can counter compensate the moving platform weight.

Unfortunately, only a single track contributes force acting on the whole moving platform at one side. This non-symmetric force system probably produces a resultant torque and an extra friction along the track during operation. Consequently, the motor would have unstable performance and become difficult to control.

On the y-axis, since the platform framework is made to be one piece, the geometry is very complicated. From the view of fabrication, a very large piece of raw material is required and much material is wasted. As a result, the motor costs a long machining time and a high manufacturing expense.

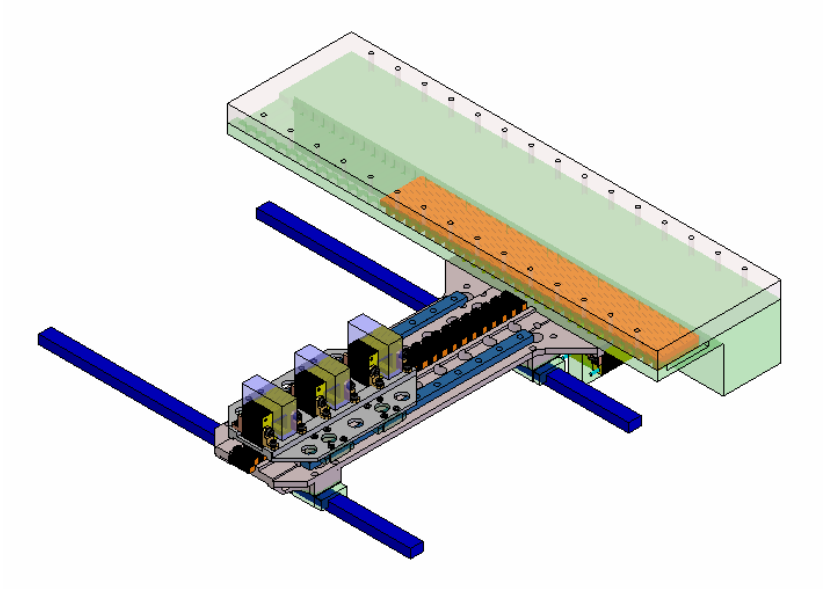

Fig. 2.2: End supported type motor.

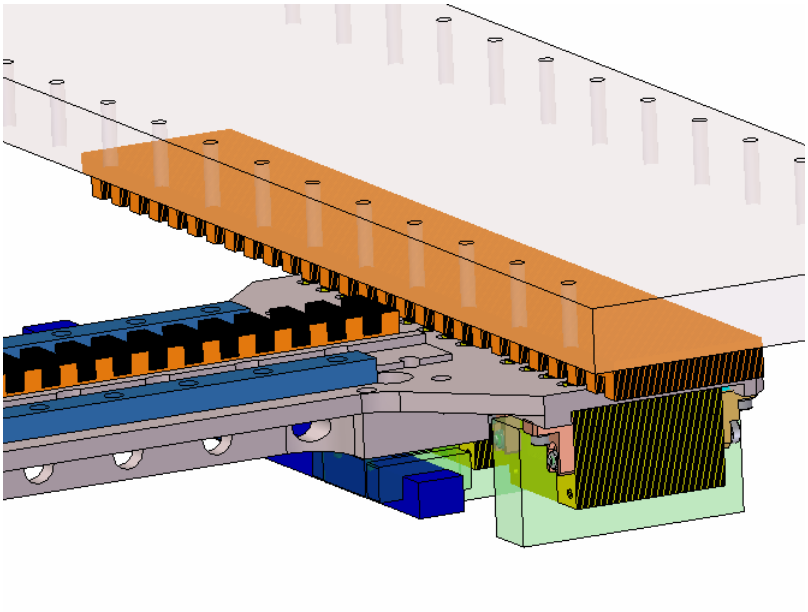

Fig. 2.3: Static track mounted above the moving platform in the end supported type motor.

2.3 Centre mounted type motor

The last motor is shown in Fig. 2.4 and described as centre mounted type since the whole x-axis motor is fixed at the centre of y-axis platform. Among the three designs, the centre mounted type motor has the smallest moving mass which is only about 1.4kg for x-axis and 5kg for y-axis. The motor is expected to achieve the highest acceleration or deceleration under the same power supply.

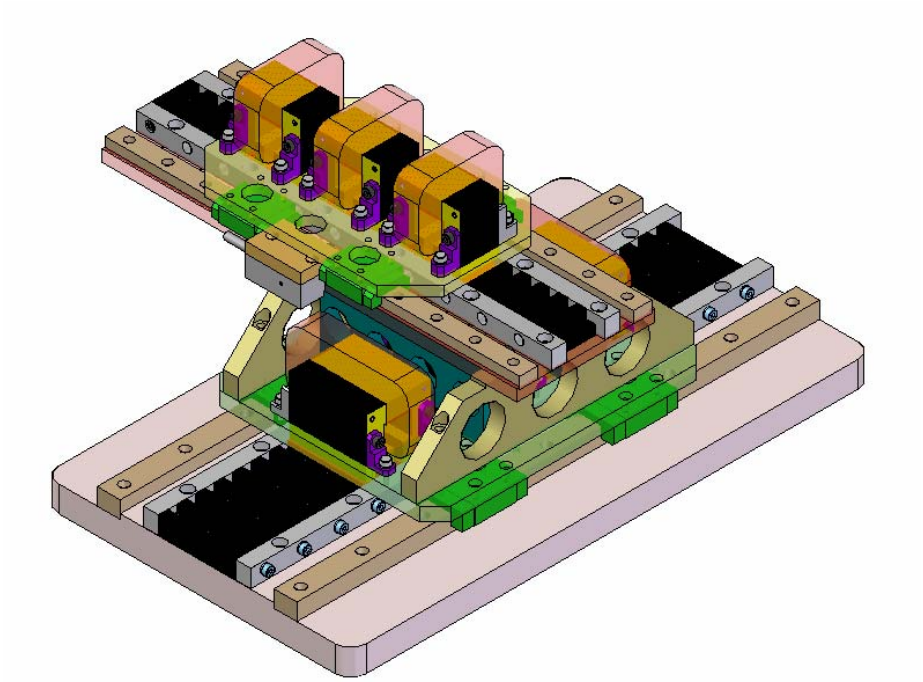

Fig. 2.4: Centre mounted type motor.

As shown in the photo, the x-axis motor is mounted on the top of y-axis moving platform. Therefore, the y-axis moving mass is much larger than the x-axis one. To solve the problem, the x-axis motor is shortened to reduce the static track mass and the laminated steel plate of the y-axis is doubled to increase magnetic field strength. Under the same applied current, the y-axis coil windings

can provide higher driving force than that in the x-axis to compensate the difference between two axis moving masses.

The whole motor framework is made of several pieces of aluminum plate to shorten fabrication time and save raw material. Each plate is drilled with holes to reduce moving mass and improve thermal dispersion. During the assembly procedure, the silicon steel laminated plates of each phase are aligned and locked together individually. The motor installation process thus becomes simpler and the maintenance procedure would be more convenient.

2.4 Summary of the advantages and disadvantages of motors

Table 2.1 and Table 2.2 summarize the advantages and disadvantages of the above three different motors. To conclude, the centre mounted type is selected as the project motor prototype.

Table 2.1: The advantages of the three types of motor design.

Motor Type	Advantages
1. Cassette Type	✓ Simple mechanical structure
2. End Supported Type	✓ Magnetic attraction counterbalances the moving mass ✓ Smaller moving mass compared to the Cassette type
3. Centre Mounted Type	✓ The smallest moving mass ✓ The shortest response time ✓ Symmetric structure ✓ High position accuracy achieved ✓ Y-axis magnetic field strengthened

Table 2.2: The disadvantages of the three types of motor design.

Motor Type	Disadvantages
1. Cassette Type	• Too heavy • Poor response time • High peak current required
2. End Supported Type	• Unbalanced model structure • Complicated mechanical framework
3. Centre Mounted Type	• Difficult to access the Y-axis coils

Chapter 3

LSRM system motion specifications

After comparing features of three different motors, the finalized LSRM is presented in this section. This chapter focuses on the motor design to achieve a better motor performance. The arrangement of the three phase coils is firstly explained and the motor data is listed out in a table. Next, the general mathematical equations of LSRM are provided.

From the view of mechanics, the motor features are highlighted and part of fabrication process is described. Different from Direct Current (DC) motor, LSRM requires “switched” current on different phase coils to drive the motor continuously. The detailed operation principle is shown with pictorial explanation.

Since the magnetic flux characteristics of LSRM are different from the typical permanent magnet motor, the next section would describe the magnetic feature at magnetic field aligned and unaligned positions. Lastly, the motion profiles for long and short traveling distance are shown and defined.

3.1 Design schematic

A three-phase coil arrangement with flux de-coupled path and 120 electrical degree separations is shown in the Fig. 3.1. They are separated with 1+2/3 pitch distance (i.e. X2=10mm). As a result, the pitch distance is designed with 12mm so as to avoid any rounding error from the division by three.

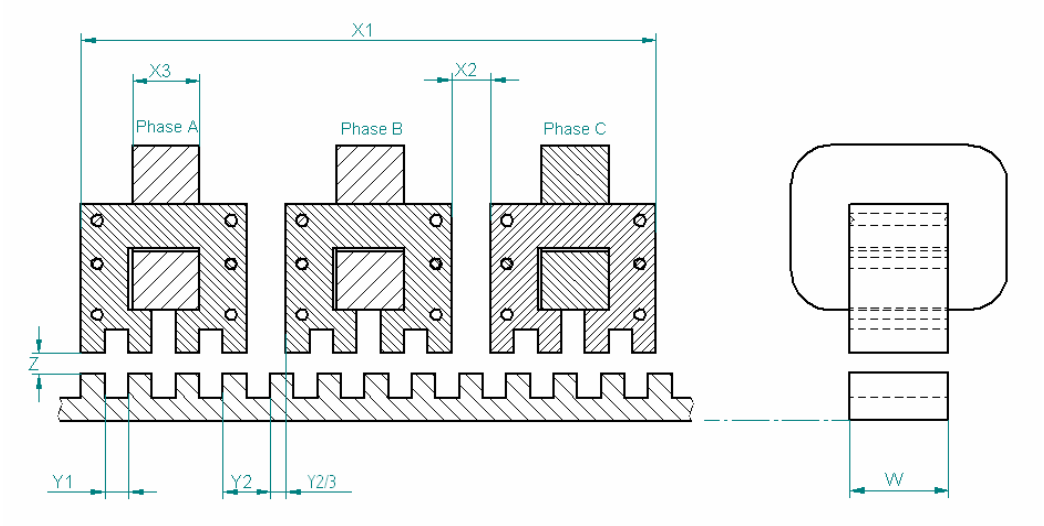

Fig. 3.1: LSRM design schematic.

For the LSRM prototype, the design of three-phase flux decoupled windings with longitudinal configuration is chosen because of following advantages.

I. The de-coupled flux windings lead to a simpler motor model due to zero mutual inductance. With this Y configuration, the mutual inductance could be self compensated.

II. The individual phase windings reduce the manufacturing cost and complexity.

III. Long travel distance can be accomplished easily by combining longitudinal track guides.

In this project, the detailed mechanical dimensions and electrical properties of the LSRM prototype are listed in Table. 3.1.

Table 3.1: LSRM characteristics.

Power Output	100 W
Maximum Traveling Distance (x)	110 mm
Moving Mass (M)	1.4 kg
Position Accuracy	±25 μm
Feedback Device	Optical Encoder with 0.5 μm resolution
Pole Width (y_1)	6 mm
Pole Pitch (y_2)	12 mm
Coil Separation (x_2)	10 mm
Winding Width (x_3)	25 mm
Air Gap (z)	0.4 mm
Number of turns per phase (N)	200
Aligned inductance	34mH
Unaligned inductance.	26mH

3.2 LSRM mathematical model

The switched reluctance linear drive system has a highly non-linear characteristic due to its non-linear flux behavior. Equation (1)-(3) present the general mathematical models of the LSRM:

$$v_j(t) = R_j i_j(t) + \frac{\partial \lambda_j(x(t), i_j(t))}{\partial x(t)} \frac{dx(t)}{dt} + \frac{\partial \lambda_j(x(t), i_j(t))}{\partial i_j(t)} \frac{di_j(t)}{dt} \quad (1)$$

$$j = a, b, c$$

$$f_e = \sum_{j=1}^{3} \frac{\partial \int_0^{i_j(t)} \lambda_j(x(t), i_j(t)) di_j(t)}{\partial x(t)} \quad (2)$$

$$f_e = M \frac{d^2 x(t)}{dt^2} + b \frac{dx(t)}{dt} + f_l(t) \quad (3)$$

where

$v_j(t)$ is the phase voltage,

$i_j(t)$ is the phase current,

$R_j(t)$ is the phase resistance,

λ_j is the phase flux linkage,

x is the travel distance,

f_e is the generated electromechanical force,

f_l is the external load force,

M is the mass and

b is the frictional constant.

3.3 LSRM mechanical features

In this project, a 1D LSRM is fabricated as shown in Fig. 3.2. The finalized x-axis motor consists of a moving platform, two pairs of Linear Motion (LM) guides, laminated steel plates at a base, a moving platform and an optical encoder. The optical encoder is used to feedback position of the translator for motion control and its resolution is 0.5μm. To improve motion control and consider manufacturing fabrication, several mechanical features are highlighted as following.

Feature One

To minimize the motor moving mass, the platform plate and the mountings are made of aluminum. Instead of material selection, holes are drilled on the plate to save the mass.

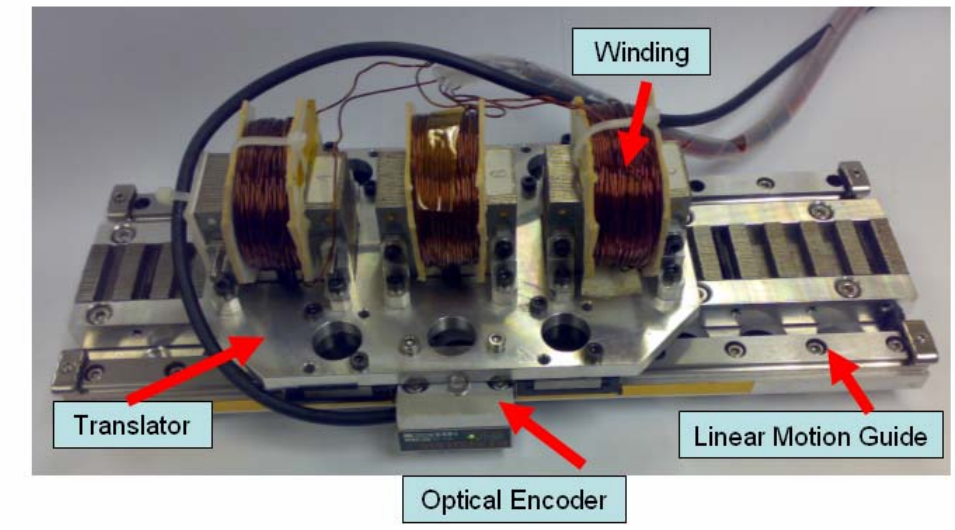

Fig. 3.2: X-axis motor construction.

Feature Two

To improve motor subassembly procedure and motor maintenance, the laminated plate is made of 0.5mm thick silicon-steel plate and every 50 pieces are grouped together. The steel plates are fabricated by punching process to allow mass production and save time. Each group of silicon-steel plate is fixed by stands on the translator and circulated by a number of wire coils. The total moving mass is about 1.4kg.

Feature Three

For each phase, a wire is deformed into a number of coils to match the shape of the laminated plate before the assembly procedure. At the same time, each laminated plate can be separated into two pieces to allow the deformed wire coil to be fit inside. Fig. 3.3 and Fig. 3.4 show that the laminated plates are aligned and locked by screw.

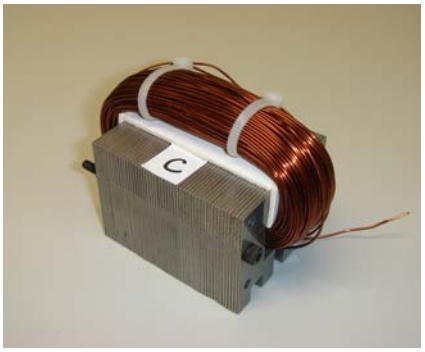

Fig. 3.3: Photo of the real coil with grouped iron plates.

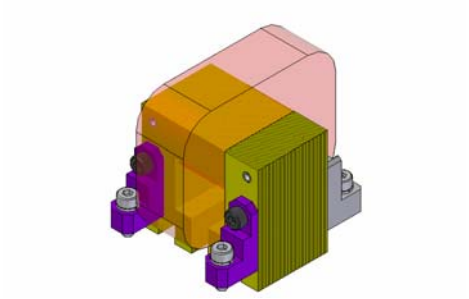

Fig. 3.4: Individual phase coil with laminated plates with mountings.

Feature Four

Three phases of coil winding are mounted on the translator instead of static track so as to minimize copper wire used and simplify the wiring connection. Similar to the moving translator, locking screws are inserted to the laminated plates to fix them on the static track as displayed in Fig. 3.5. Therefore, the steel plates would not loose out by the strong magnetic attraction from the translator or vibration motion.

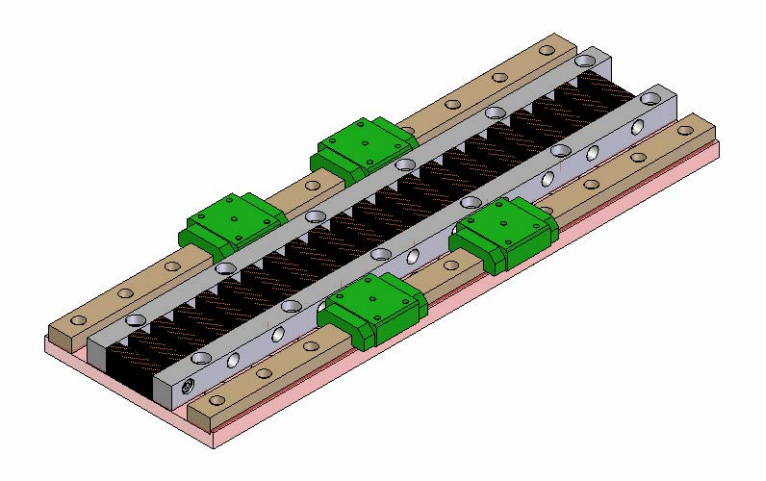

1

Fig. 3.5: Laminated plates mounted on the lower track.

Feature Five

In the motor mechanical design, the air gap between the upper moving laminated plates and the lower fixed laminated plates is inversely proportional to magnetic force generated. Minimizing the air gap is able to create the greatest driving force. In this prototype, the target air gap is 0.4mm. The grinding process in machining workshop is applied to achieve high surface flatness and keep the constant air gap. A photo is taken in Fig. 3.6.

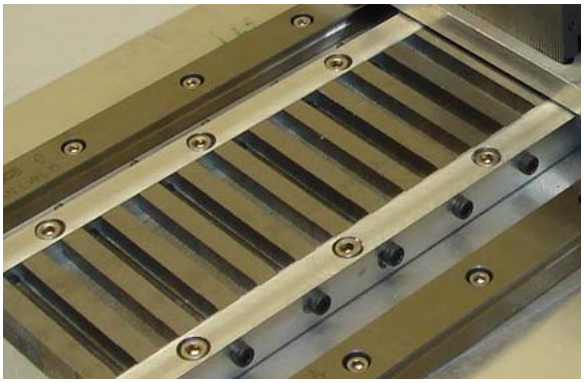

Fig. 3.6: Grinding the iron plate surface to keep constant air gap.

3.4 LSRM operation principle

For LSRM, the translator goes forward smoothly when the stator windings are switched in sequence. This section presents each motor condition with the help of figures.

Firstly, provided that only phase A coil is excited, current inside the winding will generate force to make the translator platform moves to the aligned position with the nearest stator teeth.

Secondly, the previously excited phase A will be turned off before the succeeding phase B is excited. The translator will go from the misaligned position to the next aligned position. Hence, the platform moves continually toward Left Hand Side (LHS).

Thirdly, phase C coil current takes the same role as the previous coil to move the platform to align the next teeth.

In this way, exciting the translator phase A, B & C coils sequentially drives the platform to run in LHS direction. Based on the same topology principle, Right Hand Side (RHS) motion of the translator can be achieved by reversing the excitation sequence of the stator phases. Fig. 3.7-3.9 show the position of the translator when each phase coil is excited.

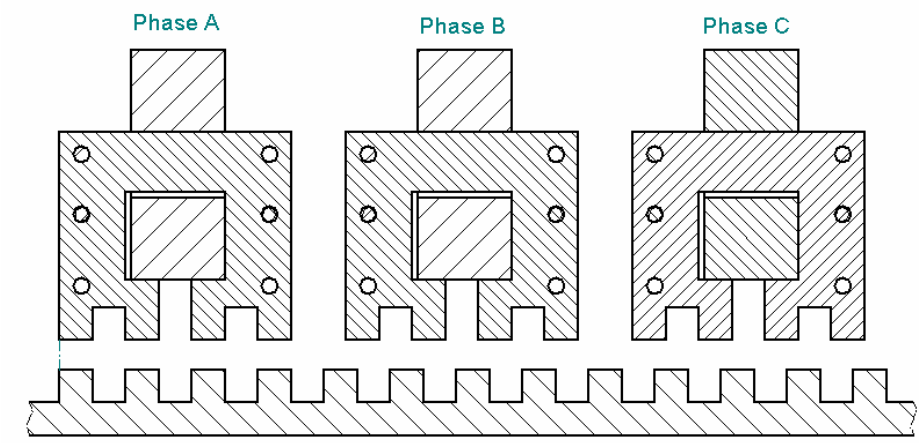

Fig. 3.7: Phase A coil excited and aligned.

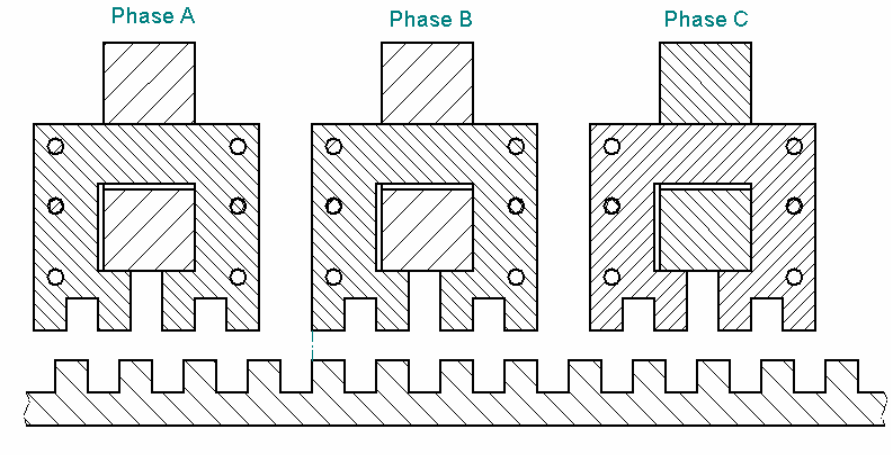

Fig. 3.8: Phase B coil excited and aligned.

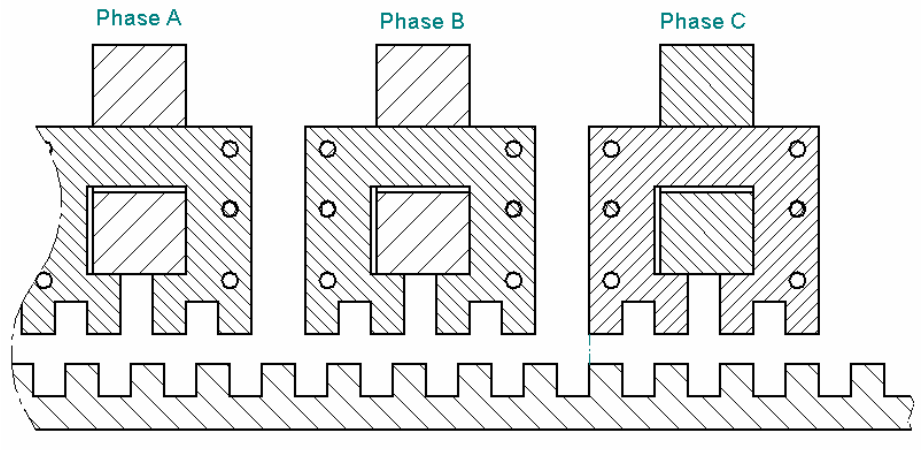

Fig. 3.9: Phase C coil excited and aligned.

As mentioned previously, when current flows through one translator winding, the exciting current tends to move the translator in such a direction as to increase the inductance, until it reaches the position with maximum inductance value.

Provided that there is no residual magnetization in the steel, the direction of the current is immaterial (i.e. unipolar). The force direction is always towards the nearest aligned position. Therefore positive force (i.e. motoring force) can be produced only if the translator is between the unaligned position and the next aligned position in the forward direction.

In other words, motoring operation can only be found in the direction of rising inductance while braking operation appears when inductance decreases. Therefore, the control of a LSRM requires a correct translator phase excitation based on the platform instantaneous position.

3.5 Flux linkage characteristics

When LSRM translator windings are excited, the current will magnetize the iron plates installed on both translator and stator. The translator platform tends to move to align itself with the magnetic flux axis of the stator phase iron plates. This position is referred to as the fully *aligned position* and has the maximum phase inductance. It is found that both the analytical and finite element results are very close to the measured inductance.

On contrary with aligned position, *unaligned position* represents the position with maximum reluctance value and hence minimum phase inductance. If translator and stator poles are evenly distributed, the unaligned translator poles will be positioned at the mid-point between two stator poles. Fig. 3.10 shows the flux linkage strength on LSRM at aligned and unaligned position.

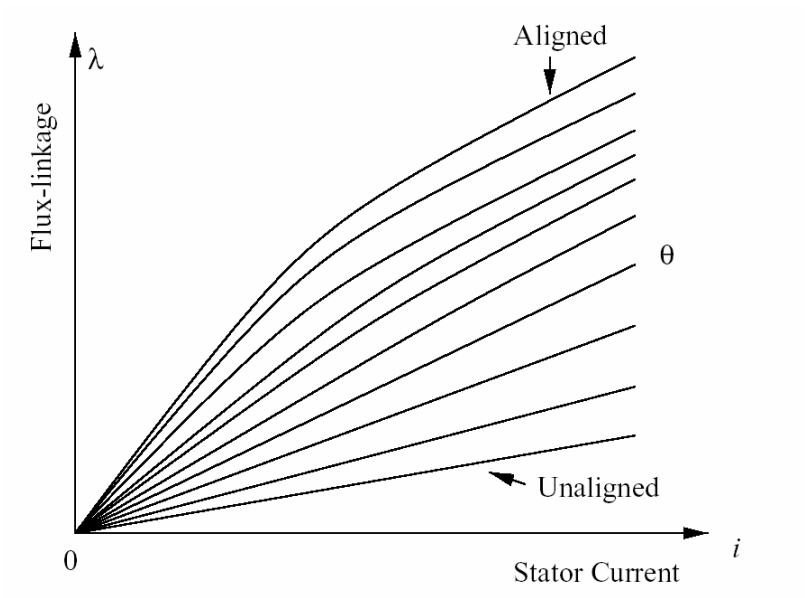

Fig. 3.10: Flux linkage on LSRM at aligned and unaligned position.

At unaligned position, a high discrepancy between theoretical and measured inductance is found. The error is attributable to the end effects and, to distortion of the magnetic properties of the core material due to punching stresses, inexact B-H characteristics provided by the steel manufacturers and non-uniformity of the air gap. Even though the end effect has been included in the analytical method, accurate modeling of the three-dimensional geometry of leakage flux tubes is difficult.

The correlation between theoretical and measured inductance will change on varying exciting current. At smaller currents, there is high correlation between the finite element analysis and measured values, but at higher currents there is a minor discrepancy between the two sets of values. For LSRM, since air gap is very large and hence no saturation appears, the inductance profiles at currents lower than the rated value are almost identical to the profile at the rated current.

3.6 Motion profiles

For precise motion control, a position tracking profile is usually prepared for position feedback control during the whole traveling motion rather than to control the endpoint accuracy. A 3rd order position S-profile with a limited input bandwidth is a typical practice to eliminate the sudden disturbance to the motor. Equation (4)–(6) govern the 3rd order S-profile generation:

$$\frac{da(t)}{dt} = \{J_{\max}, 0, -J_{\max}\} \quad (4)$$

$$v(t) = \int a(t)dt \quad (5)$$

$$s(t) = \int v(t)dt \quad (6)$$

To verify that the prototype motor is suitable for general pick and place robotic applications in semiconductor industry, 100mm motion profile is described in Fig. 3.11-3.13 and 250μm motion profile is described in Fig. 3.14-3.16. For 100mm long distance profile, maximum acceleration is $4ms^{-2}$ and maximum velocity is $0.48ms^{-1}$. The profile time is 1100ms. For 250μm long distance profile, maximum acceleration is $0.8ms^{-2}$ and maximum velocity is $0.01ms^{-1}$. The profile time is 200ms only.

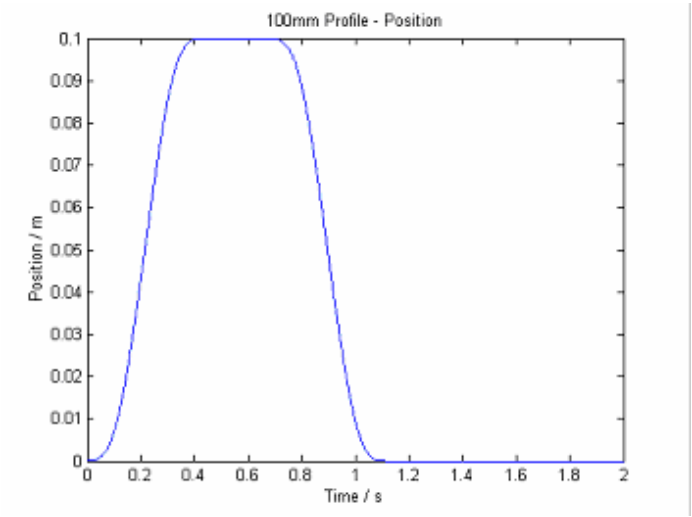

Fig. 3.11: Position profile of 100mm long distance.

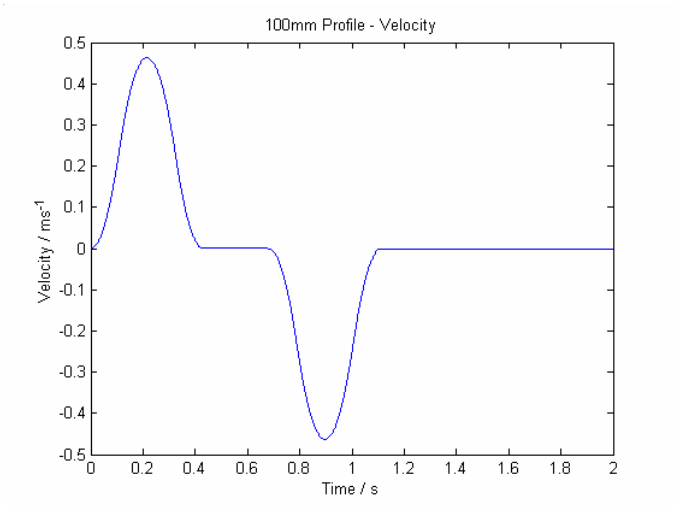

Fig. 3.12: Velocity profile of 100mm long distance.

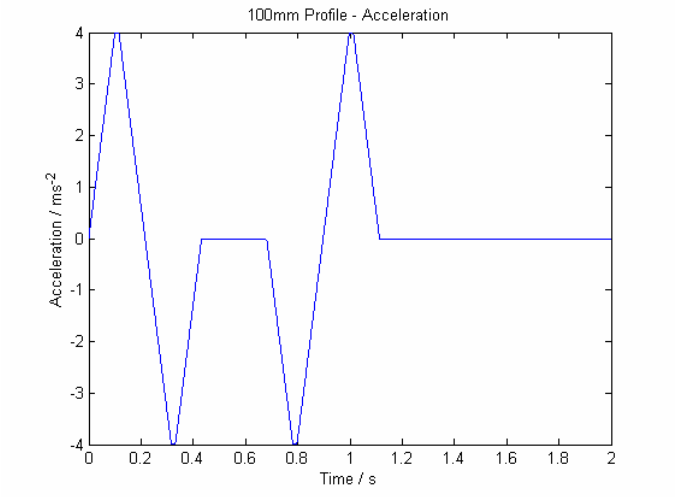

Fig. 3.13: Acceleration profile of 100mm long distance.

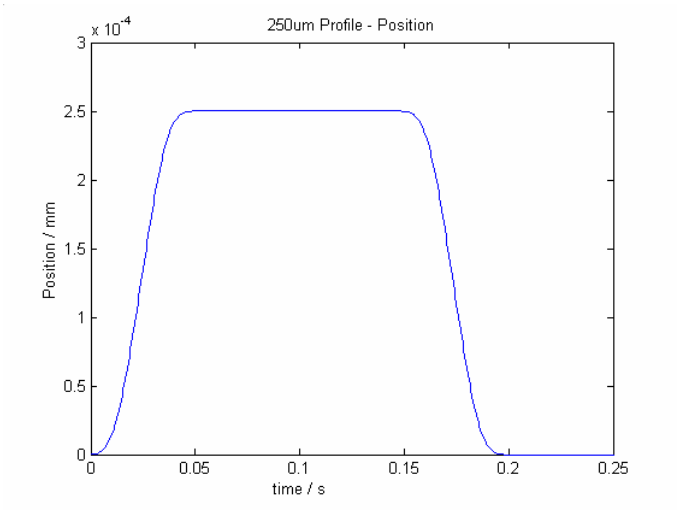

Fig. 3.14: Position profile of 250µm long distance.

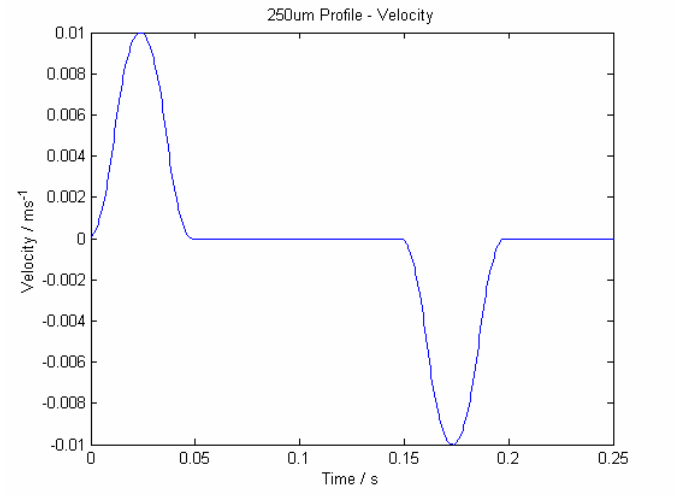

Fig. 3.15: Velocity profile of 250µm long distance.

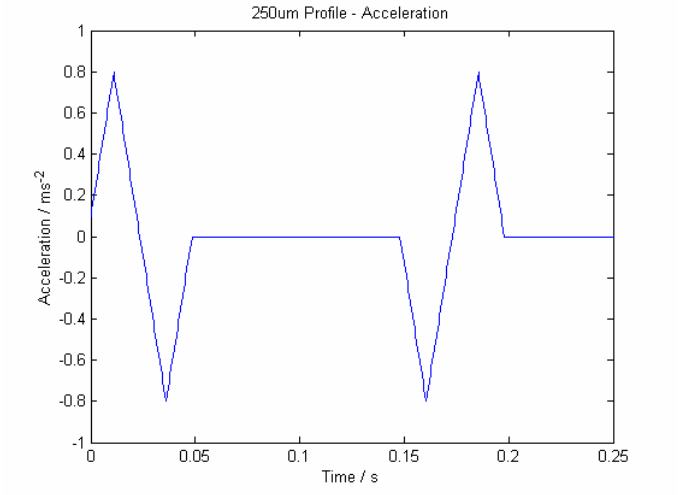

Fig. 3.16: Acceleration profile of 250µm long distance.

Chapter 4

Control system

In this chapter, the fuzzy system objective and the definition are firstly discussed in Section 4.1 and 4.2. Section 4.3 presents the advantages of fuzzy control system. Some successful applications of fuzzy controller are described in Section 4.4. After that, the comparison between conventional numerical and fuzzy controller is given in Section 4.5.

In fuzzy control system, there are four principal functional blocks which are fuzzy rule base, fuzzy interference, fuzzifier and defuzzifier. Individual component description is presented in Section 4.6. In order to shorten online computation, a look-up table fuzzification and its methodology are introduced in Section 4.7. In Section 4.8, a fuzzy controller is applied to supervise PD gain to avoid periodic fine tuning control parameters. Finally, the proposed LSRM controller structure is presented in Section 4.9.

4.1 Fuzzy logic system objectives

As a practice of intelligent controller, there are three kinds of justification for fuzzy systems theory.

4.1.1 Describe real world phenomenon precisely.

In our real world, all physical phenomenons are too complicated to provide precise and distinct descriptions. Most real systems are nonlinear. Approximation is essential in order to provide a reasonable and traceable model. In fact, fuzzy system theory can precisely present real physical phenomenon key features in a mathematical traceable manner for analysis.

4.1.2 Collect human experts' experience.

Human knowledge and experience become increasingly important for all nonlinear real system. It's required to formulate human knowledge in a systematic manner and put it into engineering systems, together with other information like mathematical models and sensory measurements. Fuzzy system can provide database to record human behavior and expert experience for theory development.

4.1.3 Combination of important information.

Generally speaking, a good engineering theory should be capable of making use of all available information effectively. For many practical systems, there are two sources of important information.

I. The first source is human experts who describe their knowledge and experience about the system in natural languages. This information cannot be described easily by a few numerical equations. It is developed through a number of practices or experiments.

II. The second source is sensory measurements and mathematical models that are derived according to physical laws. This kind of data usually is measurable and easier for data handling.

As a consequence, fuzzy system is developed to take the important task to combine these two types of information into system designs. For this achievement, human knowledge is formulated into a similar framework as used in sensory measurements and mathematical models. In other words, by the fuzzy logic system, the human knowledge and experience are transformed into mathematical formulas.

4.2 Fuzzy logic definition

In control theory, artificial intelligence is a discipline to investigate how humans solve problems and how machines can emulate intelligence problem-solving human behavior. It aims to make machines smarter by investing them with human intelligence.

By definition, the goal of using fuzzy systems is to put human knowledge into engineering systems in a systematic, efficient and analyzable order. Its main core is a collection of fuzzy IF-THEN rules. These rules are characterized by continuous membership functions. The most important advantage of fuzzy logic is to provide an effective and efficient methodology for developing nonlinear controllers in practice without using highly advanced mathematics. Therefore, fuzzy controllers do not need an explicit system model.

4.3 Advantages of fuzzy control system

For the wide application of fuzzy control system, there are several advantages.

4.3.1 Linguistic presentation

The fuzzy logic controller can be designed on the basis of the linguistic information which got from a process expert or can be designed by the process expert himself, instead of by a control expert. Therefore, the controller can be used to emulate human expert knowledge and experience. It is ideal for solving problems where imprecision and vagueness are present and verbal description is necessary. This is very useful in motor drive application where the outer control loops (speed and position loops) are more influenced by the behavior of the driven plant.

4.3.2 Simplicity

The design of the fuzzy logic controller does not require an accurate model of the plant. This is greatly appreciated in motor drive applications where the motor and the mechanical load are described by a set of nonlinear, differential equations or are partially unknown. As a consequence, its simplicity allows the solution of previously unsolved problems because they do away with complex analytical equations used to model traditional control systems.

4.3.3 Short development time

By manipulating various components of a fuzzy controller coupled with computer simulation and trial-and-error effort, a well-performing fuzzy controller can be built up easily. Rapid prototyping is possible because a system designer doesn't have to know everything about the system before starting work.

4.3.4 Low development cost

They are cheaper to make than conventional systems because they are easier to design. Since there are fewer complicated mathematical equations in the control system, the real time computation devices need not to be very powerful. Lower development cost is required.

4.3.5 High robustness

They have increased robustness. An FLC usually demonstrates better results than those of the conventional controllers, in terms of response time, settling time, and, particularly, in robustness. The latter is a worthwhile feature in motor drive applications where the mechanical load is widely varying during the operations.

4.4 Successful applications of fuzzy control

To show success of fuzzy logic control, brief descriptions of several applications are given as followings.

4.4.1 Air conditioner

The controller inside air conditioner monitors the on-off status of coolant valve, water heater valve and humidifier water valve. The control strategy uses various temperature and humidity sensors to determine how to provide a comfortable air conditioning environment in an energy-conserving way. These comfort factors are established on the basis of human experience and judgment.

4.4.2 Microwave oven

Based on measured data from the oven infrared and humidity sensors, the fuzzy logic controller computes the heating power and duration automatically. To have a delicious meal outcome, human empirical knowledge about cooking and recipes is necessary to calibrate the oven at the design stage. From the view of control, fuzzy logic is very useful to provide suitable decision to fulfill human abstract requirement.

4.4.3 DC locomotive

This is an embedded fuzzy controller developed to prevent coupler, track and motor damage during starting a heavy train. Generally, the damage is due to uncontrolled wheel slip and incorrect taking up of train slack. The fuzzy controller enhances and complements the existing conventional controller with intelligent functions derived from human driver and operator experience.

Although recent designs use choppers and Pulse Width Modulation (PWM) drives that incorporate rapid wheel slip control, literally hundreds of old resistor-technology locomotives needed to be upgraded in a cost-effective manner and an embedded fuzzy controller provided an inexpensive way.

The empirical knowledge of the most experienced human operators (i.e. train drivers) is required to calibrate and commission the system. The success of this project made it possible to extend the service life of a large number of old-technology locomotives at a low cost.

4.4.4 Induction motor controller

Induction motors are inexpensive, robust, reliable and highly efficient. However, they are difficult to control due to their complex mathematical model, their nonlinear behavior during saturation and the

oscillation of electrical parameters by temperature fluctuations. Using fuzzy logic control, the advantages include short development time, easy conversion to different motor sizes, and a large tolerance for parameter variations.

The fuzzy control block provides a constant magnetizing current which is a nonlinear function of the rotor time constant, the flux leakage factor and a non-constant offset current. Based on the shape of the magnetizing current and the range of motor parameters, the fuzzy logic system is trained to adapt its membership function and rule base.

4.5 Conventional controller and fuzzy logic controller comparison

A typical conventional controller model is shown in the Fig. 4.1. The controller starts with a mathematical model of the plant or process. Theoretically, the relationship between control parameter and process result is assumed to be linear or follow a set of derived differential equations. A number of mathematical derivation and physical prove are necessary.

Fig. 4.2 describes a more intelligent controller, the fuzzy logic controller which identifies human behavior under certain conditions. This controller needs not a deep understanding of the plant or process. Complicated mathematical model, sophisticated linear or nonlinear control theory can be saved. It implies the logical model of the thinking process used in a human operator during manipulation. Both controllers' characteristics are summarized in Table 4.1.

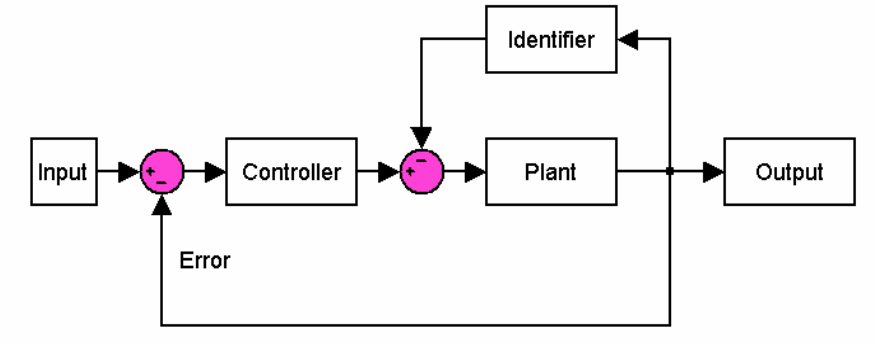

Fig. 4.1: Conventional controller.

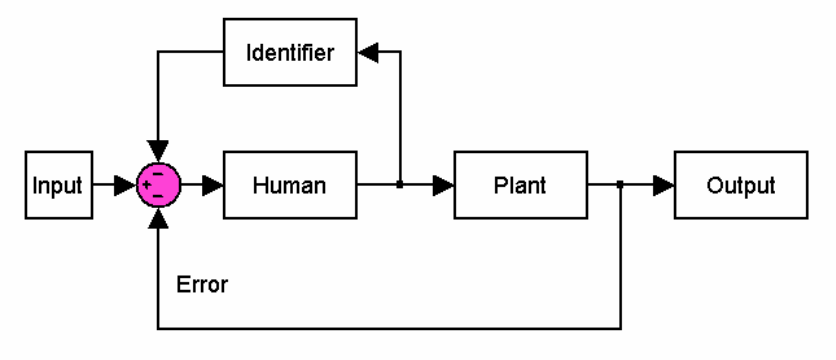

Fig. 4.2: Fuzzy logic controller.

Table 4.1: Comparisons between conventional controller and fuzzy logic controller.

Conventional controller	**Fuzzy logic controller**
1. Identify the plant or process	1. Identify the human behavior
2. Start with mathematical models	2. Start with human expertise
3. Assume defined relationship between control parameter and process result	3. No assumption

4.6 Fuzzy control mechanism

A fuzzy system is a knowledge-based or rule-based system. The starting point of constructing a fuzzy system is to obtain a collection of fuzzy IF-THEN from human experts. The next step is to combine these rules into a single system.

To construct a knowledge based system from human experience in the form of fuzzy IF-THEN rules, there are three procedures.

1. Investigate the real system to define input variables (condition) and output variables (action).
2. Derive IF-THEN rules based on linguistic expression.
3. Practice in the real system to fine-tune parameter to achieve satisfied performance.

Shown in Fig. 4.3, a fuzzy system consists of four principal functional blocks which are fuzzy rule base, fuzzy interference, fuzzifier and defuzzifier. This controller structure represents a transformation from the real-world domain using real numbers to the fuzzy domain which has a fuzzy inference engine for decision-making. Lastly, an inverse transformation from the fuzzy domain into the real-world domain is given.

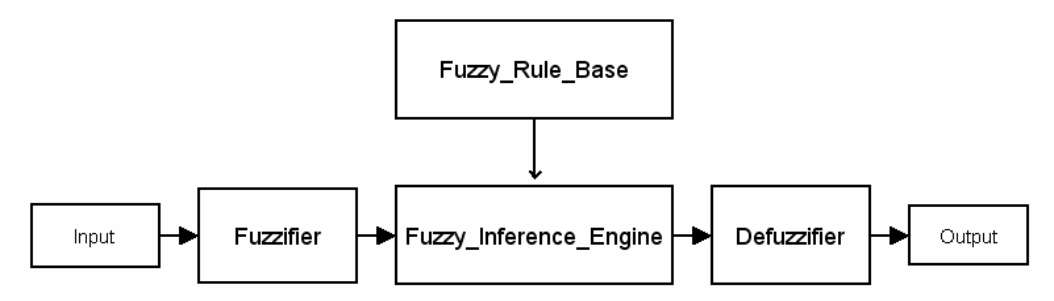

Fig. 4.3: Fuzzy control mechanism.

4.6.1 Fuzzifier

Defined by membership functions, a fuzzifier translates real valve variables or linguistics values to fuzzy input valves for a fuzzy inference engine. Since a large range of values are grouped into a few fuzzy categories, computing processes are simplified. There are generally three types of fuzzifier which are singleton, Gaussian and triangular fuzzifier. The singleton fuzzifier is the simplest while the Gaussian fuzzifier is applied for smooth performance. They are shown in equation (7) and (8).

A. Singleton fuzzifier

$$\mu(x) = \{1 \text{ if } x=x^* \text{ and } 0 \text{ otherwise}\} \quad (7)$$

where x is input variable.

B. Gaussian fuzzifier

$$\mu(x) = e^{-(\frac{x_1-x_1^*}{a_1})^2} \Gamma \ldots\ldots \Gamma e^{-(\frac{x_n-x_n^*}{a_n})^2} \quad (8)$$

where a_i are positive parameters and the t-norm Γ is chosen as algebraic product or min.

4.6.2 Fuzzy rule base

A fuzzy rule base consists of a set of fuzzy IF-THEN rules which represent human knowledge and experience. These fuzzy rules expressed in linguistic terms are defined in numeric terms in a database. This database consists of a graphical numeric function that assigns fuzzy membership values into the maximum amplitude of 1 over its universe of discourse.

For example,

IF the speed of a car is high, THEN apply less force to the accelerator.

Generally, the most popular membership function shapes are triangles and trapezoids because they are the simplest and easiest to generate. In case that a smooth performance is highly requested, Gaussian function is selected.

4.6.3 Fuzzy inference engine

Governed by the fuzzy rules and a set of conditions, a fuzzy inference engine uses fuzzy implications to simulate human decision-making. It enquires the fuzzy input valves to determine fuzzy output valves.

4.6.4 Defuzzifier

A defuzzifier generates a single numeric valve that best represents the inferred fuzzy values of the linguistic output variable.

Center-of-Area (CoA) defuzzifier is defined to calculate the centroid of the composite area representing the output variable membership functions. CoA is the most commonly used due to its continuity and simplicity. In closed loop control system, continuous methods are recommended since any sudden changes or jumps in the controller output would create system instabilities. By membership function of *B'*, equation (9) governs CoA, *y**

$$y^* = \frac{\int_V y\mu_{B'}(y)dy}{\int_V \mu_{B'}(y)dy} \qquad (9)$$

where $\int_V$ is the conventional integral and where *y* is output variable.

4.7 Table look-up fuzzification

In the fuzzy system applied in the LSRM controller, the fuzzification and defuzzification require a real time computing on membership function equations. To shorten computation time, a table look-up fuzzification technique is investigated. In [13], the table look-up representation of the fuzzy rule base is applied and observed that the final control performance is indistinguishable from that of the pure neural network controller and even provide more successful result in some cases.

The table look-up scheme involves five steps to design the fuzzy system:

Step 1

Normalize input and output valves on their whole possible range.

Step 2

Pre-calculate the membership valves from 0 to 1 to generate rules from input-output pairs. Fig. 4.4 shows the different membership valves for two-inputs and one-output case. From the pair $(x_{01}^1, x_{02}^1, y_0^1)$, the IF-THEN rule should be :

IF x1 is B1 and x2 is S1, THEN y is CE.

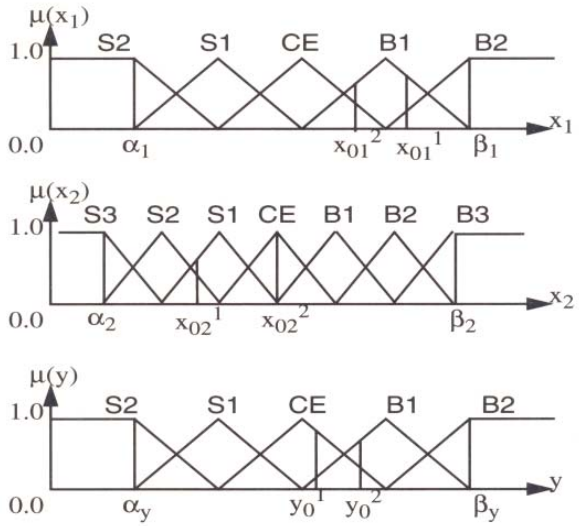

Fig. 4.4: Membership functions of input-output pairs.

Step 3

Assign a degree to each rule generated from the input-output pair in Step 2 based on the following equation.

$$D(rule) = \mu_{B1}(x_{01}^1)\mu_{S1}(x_{02}^1)\mu_{CE}(y_0^1) \qquad (10)$$

Step 4

Create fuzzy rule base by inserting the valves into discrete look-up table cells which represent input and output valve relationships. Fig. 4.5 is the example of look-up table.

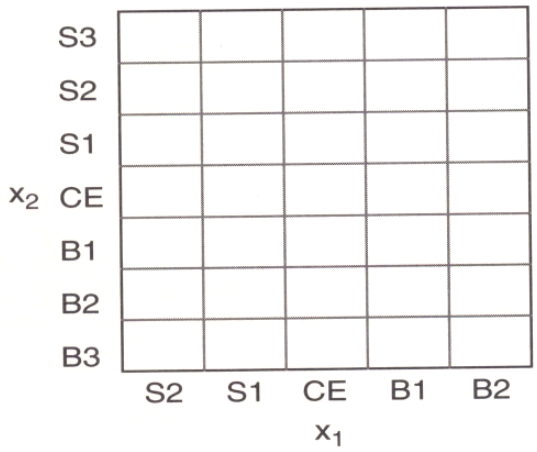

Fig. 4.5: Table look-up illustration of the fuzzy rule base.

Step 5

Apply interpolations shown in Fig. 4.6 for those input valves between the discrete cells. Instead of fuzzifying the discrete variables on line, the fuzzified values are proposed to be looked up by interpolating between the discrete values if the input values fall outside the grid.

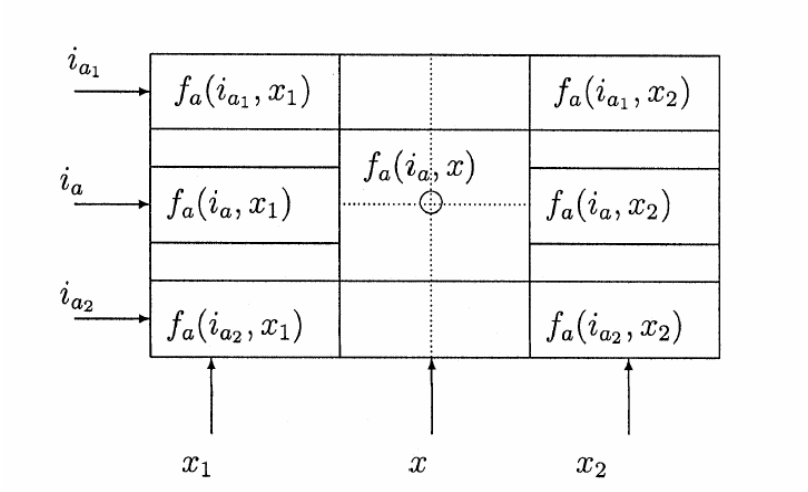

Fig. 4.6: Interpolating f_a from fuzzified table.

For the inputs $f_a(i_{a_1}, x_1), f_a(i_{a_2}, x_2), f_a(i_{a_1}, x_2), f_a(i_{a_2}, x_2)$ where $i_{a_1} \le i_a \le i_{a_2}$

and $x_1 \le x(t) \le x_2$. The two intermediate values can be found using following equations.

$$f_a(i_a(t), x_1) = f_a(i_a(t), x_1) + \left(\frac{i_a(t) - i_{a_1}}{i_{a_2} - i_{a_1}} \right) [f_a(i_{a_2}, x_1) - f_a(i_{a_2}, x_1)] \quad (11)$$

$$f_a(i_a(t), x_2) = f_a(i_a(t), x_2) + \left(\frac{i_a(t) - i_{a_1}}{i_{a_2} - i_{a_1}} \right) [f_a(i_{a_2}, x_2) - f_a(i_{a_2}, x_2)] \quad (12)$$

Finally, the output force value can be computed by

$$f_a(i_a(t), x(t)) = f_a(i_a(t), x_1) + \left(\frac{x(t) - x_1}{x_2 - x_1} \right) [f_a(i_a, x_2) - f_a(i_a, x_1)] \quad (13)$$

Since fuzzy rule calculation is done offline, only interpolation is applied in real time operation to replace complicated fuzzification and defuzzification computation. Process time is shortened to achieve faster response. At the same time, table construction approach is much simpler than maintaining a number of fuzzy rules. From the view of investment, the hardware cost is reduced due to less demanding on high speed real time processing. Consequently, table look-up fuzzification is economic and the approach is highly proposed.

4.8 Fuzzy logic PD supervisory controller

In a complex practical system, single loop control systems may not effectively achieve the control objectives but a multi level control structure turns out to be very helpful. In this project, the multi level controller is proposed. The lower level controller performs fast direct control and the higher level controller performs low speed supervision.

In industry, the majority of robotic feedback controllers are using Proportional-Integral- Differential (PID) controllers. Depends on the process or plant behavior required, PID controllers determine the best mutual adjustment of fixed weighing constants

$$i = Kp * x + Kd * \frac{dx}{dt} + Ki * \int x dt \qquad (14)$$

where

Kp is the proportional gain to improve the sensitivity to parameter variations.

Ki is the integral gain to improve the steady-state accuracy.

Kd is the derivative gain to improve the stability of the system by increasing the damping.

For a fast response and accurate robot application, the robot arm would not stay at the end point for long time and the static error is very small. Majority of the position error accumulate from dynamic error. Therefore, *Ki* is not

considered in feedback control.

Unfortunately, PD controllers work under the assumption of linear error functions. If the process input-output relationship is nonlinear, periodic tuning of the controller parameter is required. Therefore, fuzzy control is proposed to take a role to supervise PD gain parameters instead of fine tune the parameters periodically. The motor controller robustness is greatly improved.

Fig. 4.7 shows the proposed controller architecture. The first level is PD controller and the second level fuzzy system adjusts the PD parameters according to certain heuristic rules. In this supervisory controller, the profile distance is the input variable while the position gain and the velocity gain are the output variables.

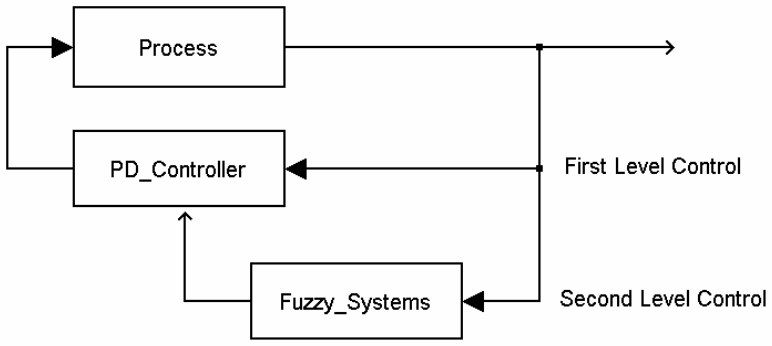

Fig. 4.7: Fuzzy supervising PD controller.

4.9 The proposed controller of the whole LSRM system

Applying the table look-up fuzzification in the inner control loop to represent the force and current relationship and supervising the feedback parameters (position gain and velocity gain) in the outer position loop by fuzzy logic controller, the integrated controller for the whole LSRM system is proposed in Fig. 4.8. Comparing with the conventional numerical controller, the real-time processing can be improved and the motor becomes more robust over a wide range of traveling applications.

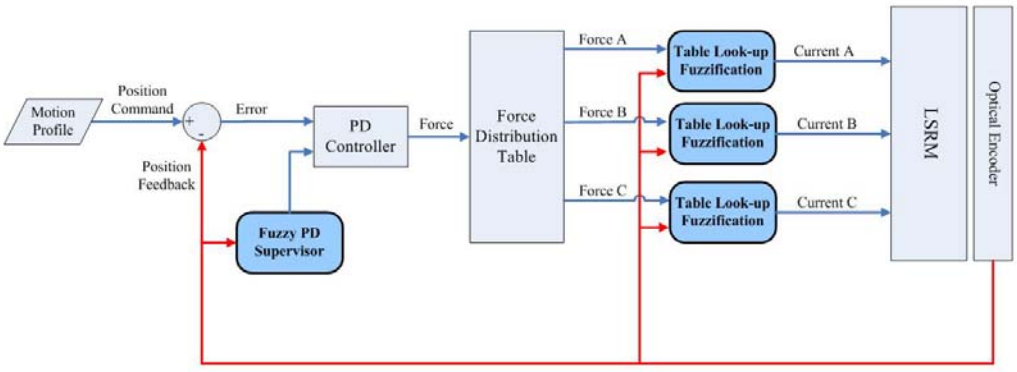

Fig. 4.8: The proposed controller of the whole LSRM system.

Chapter 5

Results

After presenting LSRM system specifications and explaining the control principle. A series of experimental results are provided for evaluation. In the beginning, the experiment setup is described with photos taken in the laboratory. The second section spends effort to calculate motion control parameters.

Based on the force feedback measured on the real LSRM prototype, the proposed current force controller is shown. With the help of Simulink software, the simulation provides useful information to prove the success of the proposed controller.

In order to consider the mechanical uncertainty in the prototype, real experiments are taken for confirmation. Beside the inner control loop, another fuzzy controller is proposed for outer PD control loop and the experimental result is shown as well.

For both simulation and real experiment, long and short traveling distances are studied to cover the whole LSRM prototype capable moving distance. Finally, a summary of the LSRM position accuracy improvement is given.

5.1.Experimental setup

In this project, in order to implement the proposed control algorithm on LSRM, dSPACE is selected as the hardware interface between the host Personal Computer (PC) and the controller. Apart from hardware, software used includes Matlab/Simulink and ControlDesk. The whole LSRM control diagram is shown in Fig. 5.1.

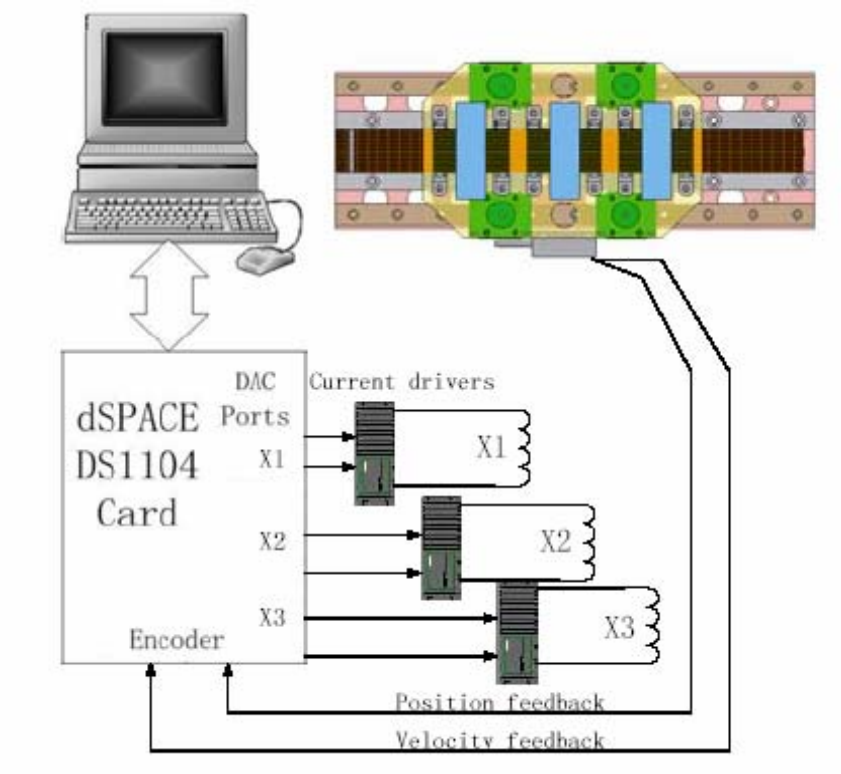

Fig. 5.1: The whole LSRM control diagram.

With the use of Simulink software, the motion control program is initially written for simulation which could only provide the theoretical result. Therefore, a series of experiments will be taken to evaluate the simulation results and proposed control algorithm.

Before motion tests, the program is firstly complied and saved in dSPACE card for real time computing. During experiments, ControlDesk software controls online parameter settings and collects instantaneous motor data such as position, velocity, acceleration and current applied. At the same time, the dSPACE card hardware provides computed output voltages to control motion drives to provide exciting current for coil windings. Then, the measured translator position error can be used to compare different control algorithms.

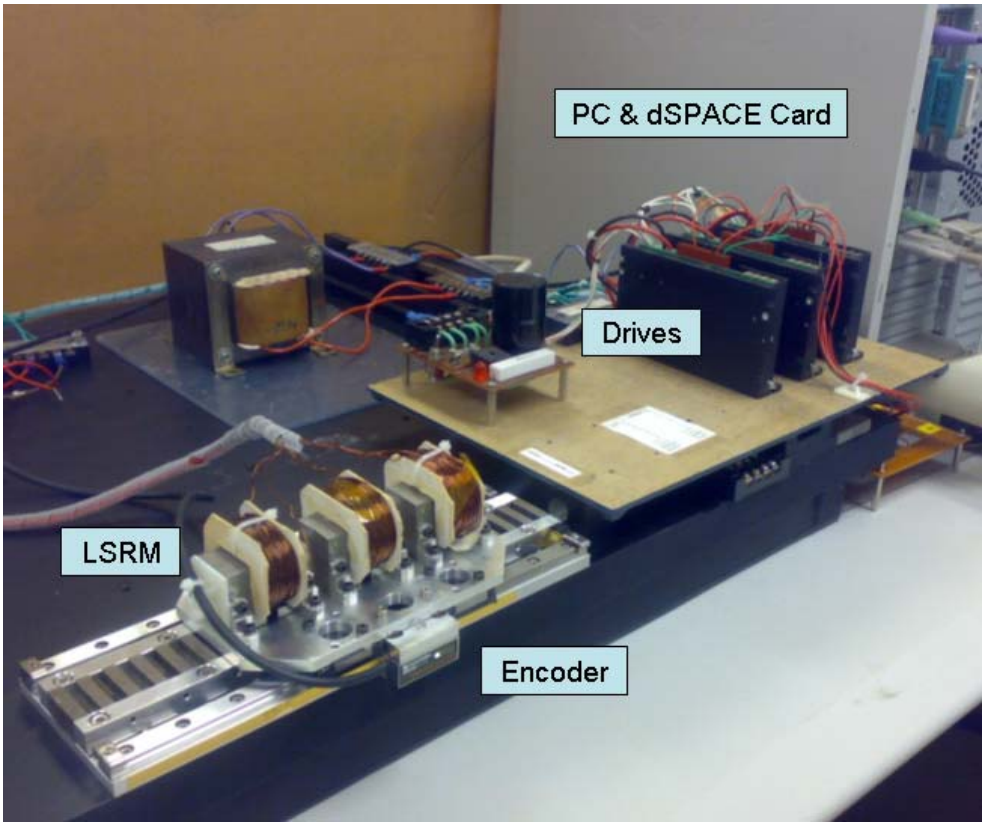

Fig. 5.2: The LSRM prototype and the control hardware setup in the laboratory.

Based on the key modules, LSRM and drives, the prototype setup in the laboratory is shown in Fig. 5.2 and the components are listed as below:

1. A LSRM prototype.

2. A Pentium IV PC.
3. A dSPACE Card. (Model no. DS1104)
4. A transformer.
5. Three AMC PWM drives (Model no. 25A8)
6. A Renishaw encoder (Model no. RGH24Z)
7. A load cell (Model no. ELFS-T3M-50N)

Firstly, a Pentium IV personal computer is used with a dSPACE card (DS1104) for control diagram constructing, program compiling and motion control in real time operation.

To provide motor power, three PWM drives (25A8) with peak current 25A are applied to vary input current for three different coils. Due to the motor nature characteristics, there are three different phases of winding coil to be controlled by individual drives. In addition, the exciting current should be provided with ‘switched’ patterns in order to drive the LSRM to run smoothly along the track.

For the translator position feedback, a Renishaw encoder (RGH24Z) with 0.5μm resolution is used as the sensing device.

During operation, the position controller applies the sampling frequency in 2kHz because it can cover most of the significant mechanical vibrations.

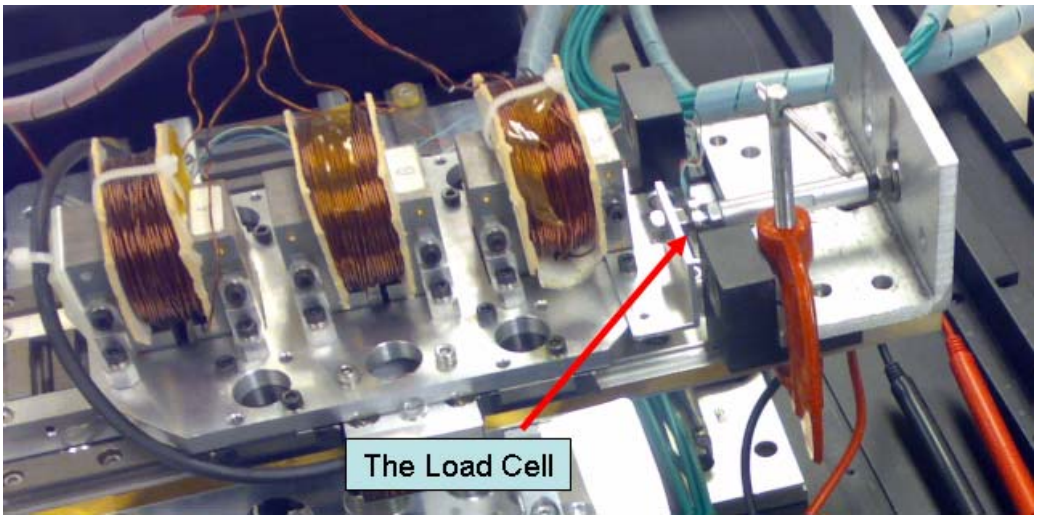

Fig. 5.3: The LSRM force measurement setup.

Fig. 5.4: The load cell.

In order to know the real LSRM force characteristics, Fig. 5.3 shows the measurement setup and Fig. 5.4 provides the photo of the load cell which is used as a force gauge to measure the force generated along the track under varying applied currents.

5.2 Calculation of control parameters

Since LSRM is usually applied on continuous series motions, very short settling time is expected and the integral component can be ignored. The whole LSRM position controller can be simplified to be a closed loop control system with PD gain only and presented in Fig. 5.5.

By employing transfer function, the outer loop control parameter K_P and K_D can be calculated with the frictional characteristics of the motor. These frictional parameters can be measured from the real model and the valves are found as below.

1) Static friction = 0.5N
2) Frictional constant, b = 0.4kg/ms^{-1}
3) Average motor force constant, K_m = 4N/A.

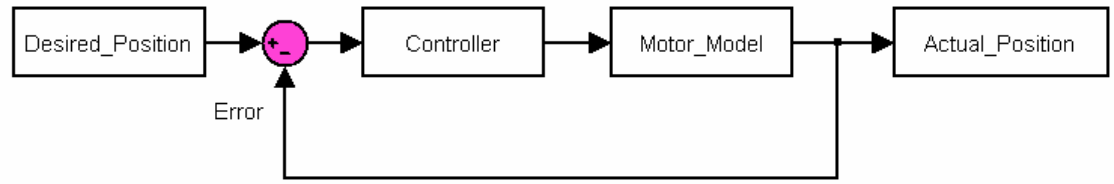

Fig. 5.5: Simplified control system.

For a PD feedback controller,

$$G_C = K_P + K_D s \tag{15}$$

To simplify the calculation, LSRM is assumed to be 2nd order function.

$$G = \frac{K_m}{s(Ms + b)} \tag{16}$$

$$G = \frac{4}{s(1.4s + 0.4)}$$

Transfer function = Actual position / Desired position

$$T(s) = \frac{G_C G}{1 + G_C G} \tag{17}$$

$$T(s) = \frac{2.6K_D s + 2.6K_P}{s^2 + (K_D + 0.007)2.6s + 2.6K_P}$$

The deadbeat system approach is employed to solve the transfer function. Settling time, T_s is set to be 25ms. Constant, ω_n is 193. Based on 2nd order function,

$$T(s) = \frac{\omega_n^2}{s^2 + 1.82\omega_n s + \omega_n^2} \tag{18}$$

$$s^2 + 351s + 37249 = 0 \tag{19}$$

$$K_P = 14200$$

$$K_D = 135$$

5.3 Proposed current force controller

Before comparing the performance of the conventional numerical controller and the proposed controller, simulations are done with two different controllers individually to verify the result shortly. The simulation framework is shown is Fig. 5.6 and LSRM model blue box will use the previously measured force distribution in the real LSRM.

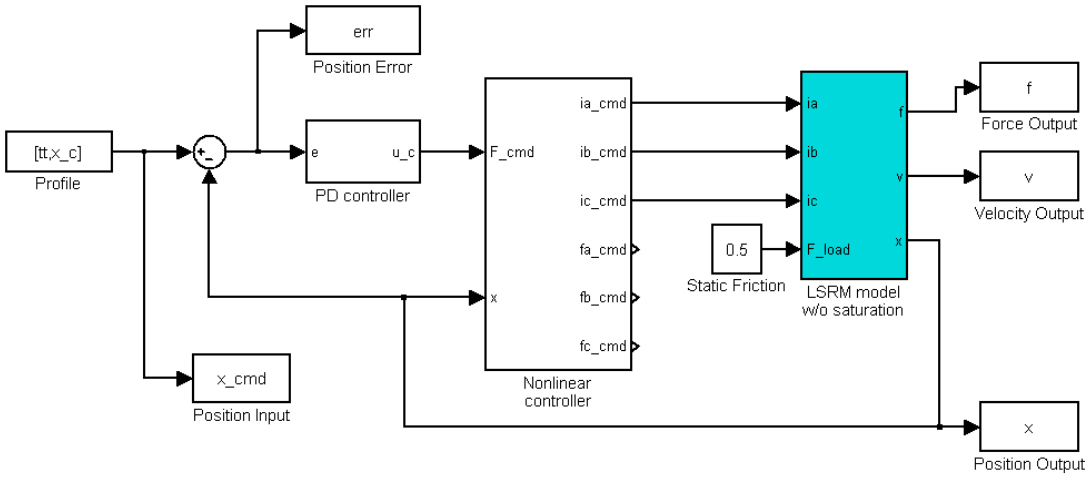

Fig. 5.6: LSRM simulation diagram using the actual force measurement.

For the numerical approach in the force-current controller, it is assumed that the force output is proportional to the square of exciting current. The magnetic force changes at different positions and thus a sine function is used to represent the force behavior along the motor teeth. The force distribution is shown in the following figures.

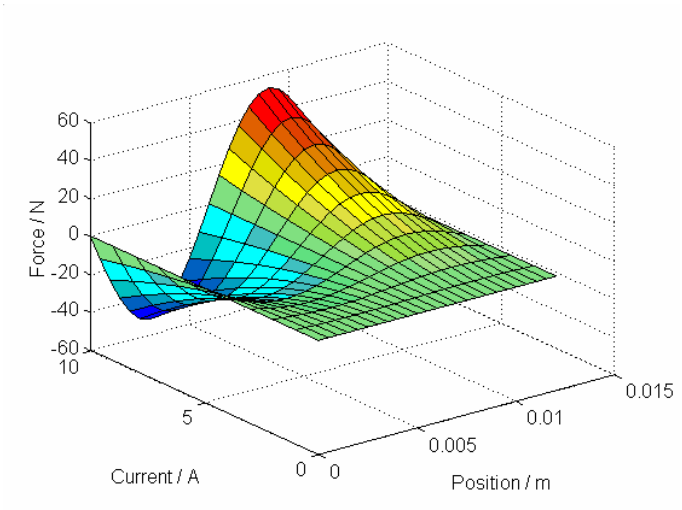

Fig. 5.7: 3D curve of theoretical force against position and current.

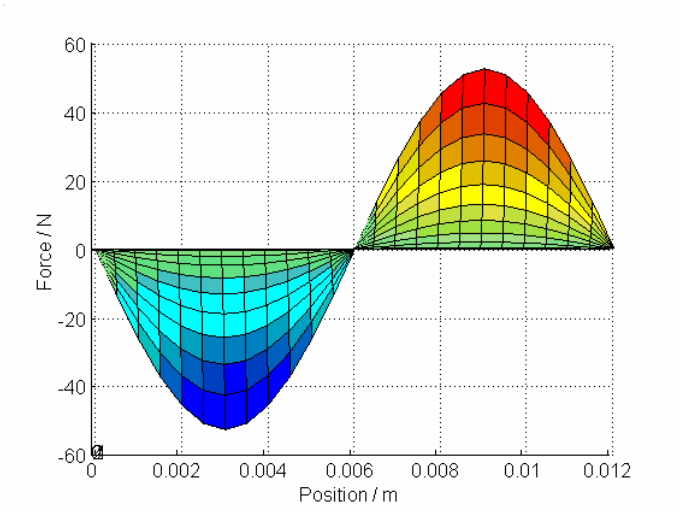

Fig. 5.8: Theoretical force against position.

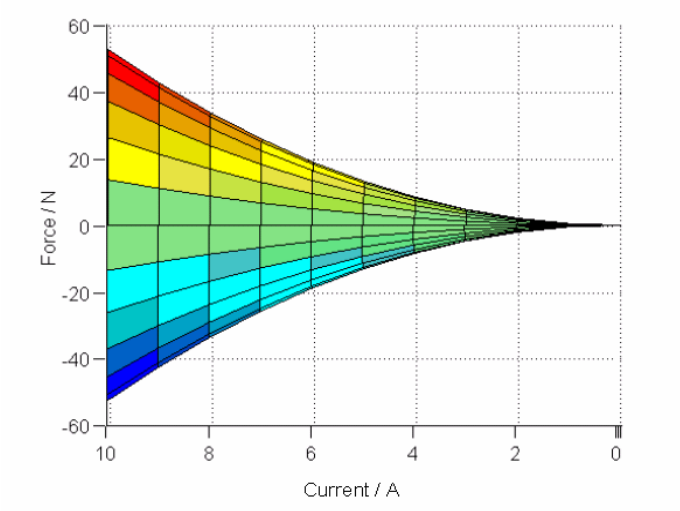

Fig. 5.9: Theoretical force against current.

From the measurement results in Fig. 5.10-5.12, the force output is only proportional to the square of current when the current is under than 2A. In case that the current is higher than 4A, the force output becomes linearly proportional to the current valve. The theoretical assumption is applicable for exciting current below 2A. In the proposed fuzzy controller, the current output is adjusted to follow linear proportional relationship when current is high.

Along the motor teeth direction, asymmetrical force distribution is discovered. This phenomenon is caused by the end effect of the motor teeth corner. Since the partial magnetic flux escapes at the laminated metal plate corner, the magnetic field and hence the generated force become weaker. In the proposed fuzzification look-up table controller, higher current will be given to compensate the magnetic flux loss. Similar to the theoretical force distribution, the proposed force current controller is presented in Fig. 5.13-5.15.

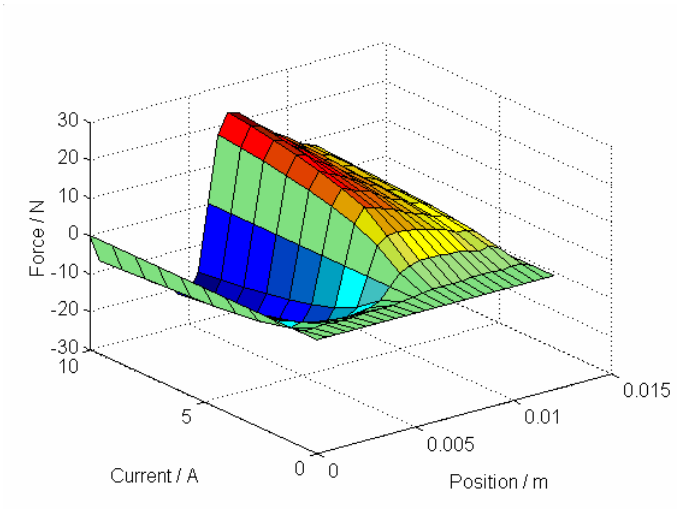

Fig. 5.10: 3D curve of actual force against position and current.

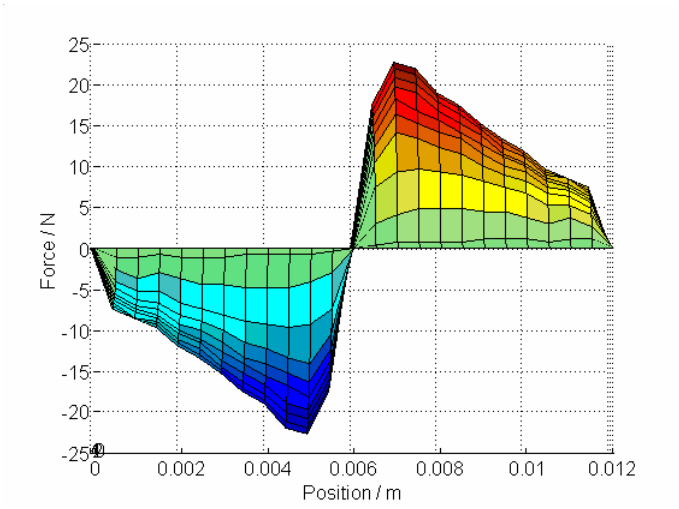

Fig. 5.11: Actual force against position.

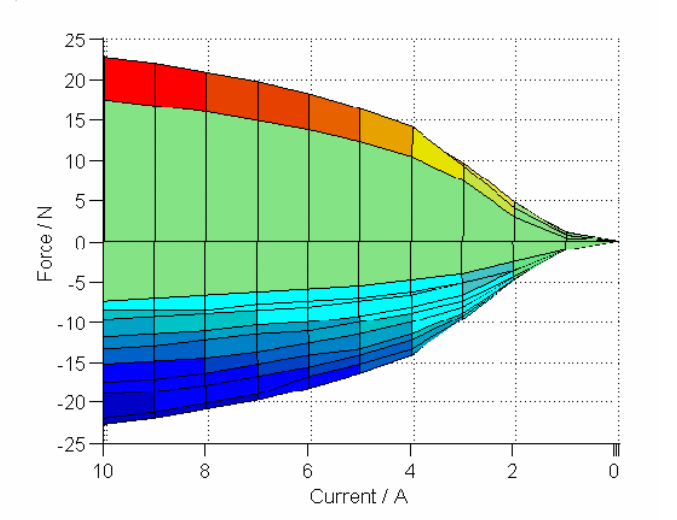

Fig. 5.12: Actual force against current.

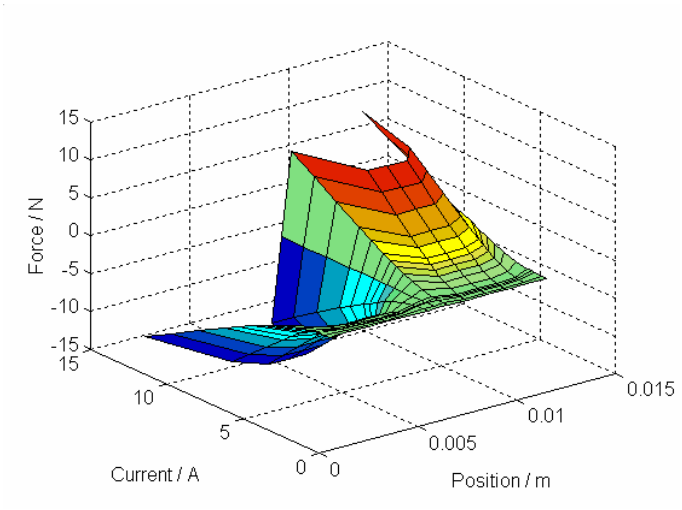

Fig. 5.13: 3D curve of force against position and current in the proposed controller.

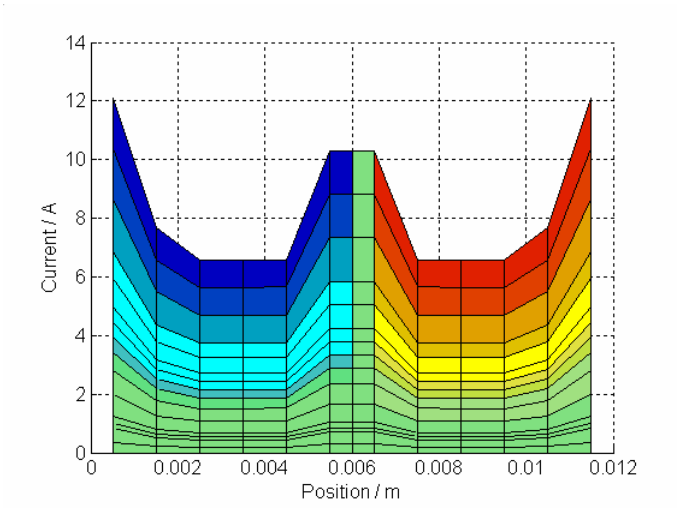

Fig. 5.14: Force against position in the proposed controller.

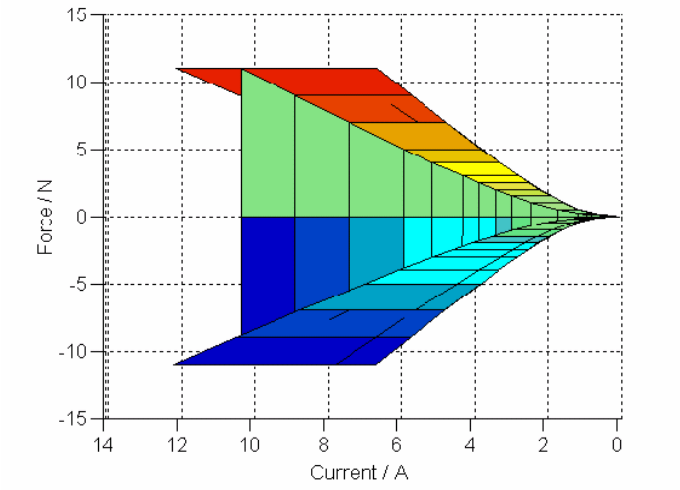

Fig. 5.15: Actual force against current in the proposed controller.

5.4 Simulation result

Before the motion test on the real prototype, the Matlab simulink software is applied to simulate the motor performance with different controllers. Assuming constant static friction and dynamic frictional gain, a long distance (100mm) and a short distance (250μm) traveling simulations are done.

Both of position and velocity feedback gain (K_P, K_D) are kept constant in the experiments to ensure fair comparisons. For the long distance profile (i.e. 100mm), the position gain is 14200 and the velocity gain is 135. For the short distance profile (i.e. 250μm), the position gain is 30000 and the velocity gain is 100.

5.4.1 Long distance (100mm)

For long distance (100mm) simulation, Fig. 5.16 shows that maximum dynamic error range is 0.35mm with the conventional controller. Appling the proposed controller, the error range is reduced to 0.16mm in Fig. 5.19 whereas the peak current is below 3.1A in Fig. 5.20. The improvement is around 54%. The maximum dynamic error is found at the highest acceleration and deceleration. The peak current and thus the greatest force are required accordingly.

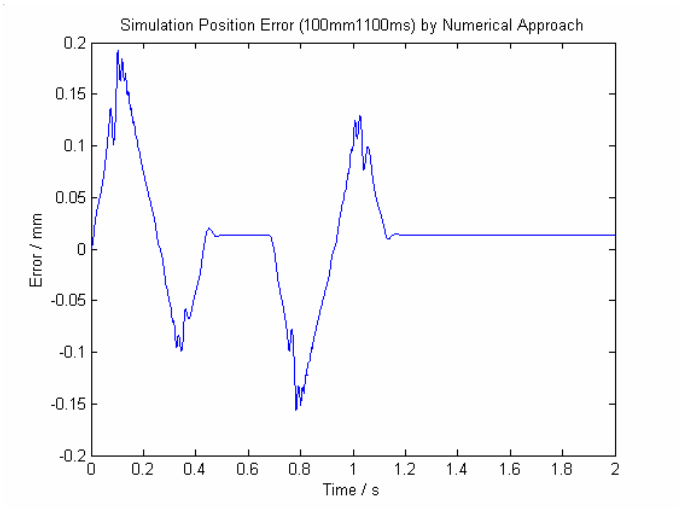

Fig. 5.16: Position error simulated by numerical approach on 100mm.

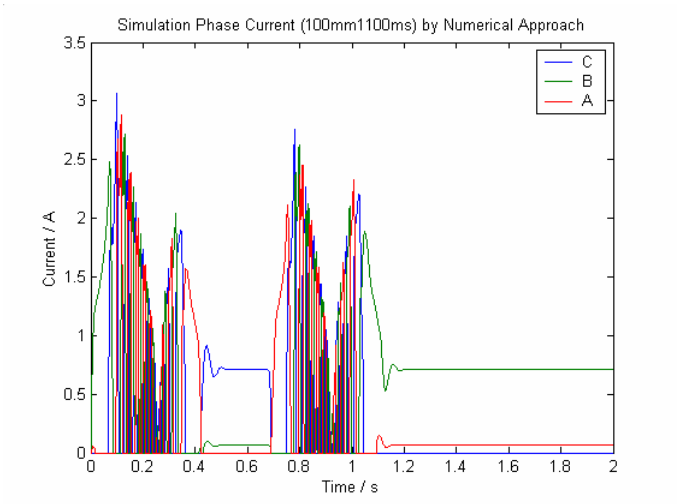

Fig. 5.17: Phase current simulated by numerical approach on 100mm.

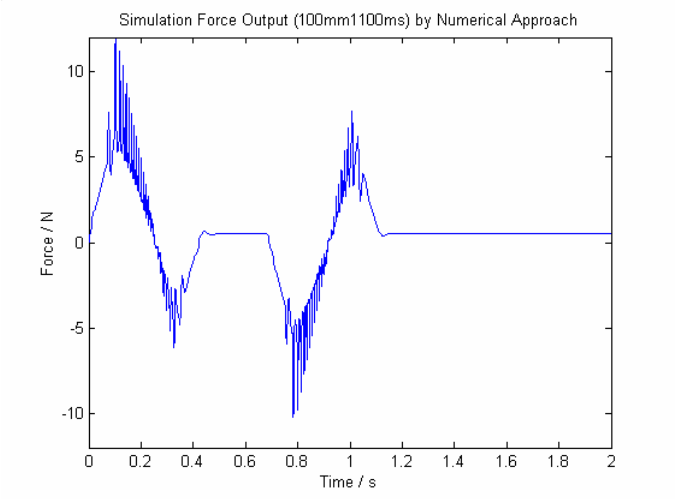

Fig. 5.18: Force output simulated by numerical approach on 100mm.

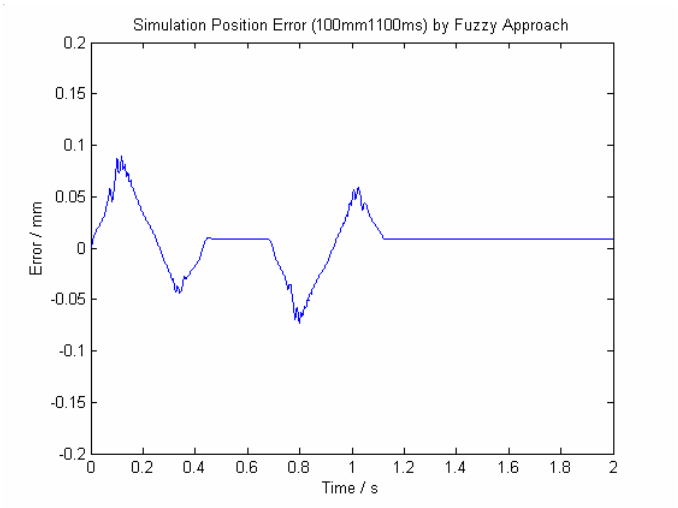

Fig. 5.19: Position error simulated by proposed controller on 100mm.

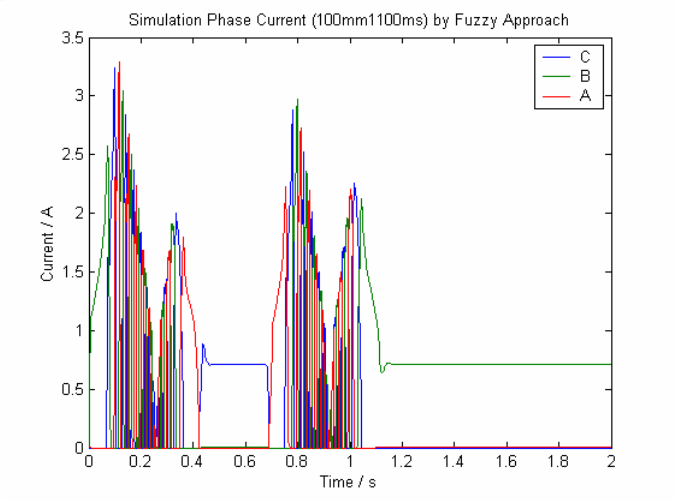

Fig. 5.20: Phase current simulated by proposed controller on 100mm.

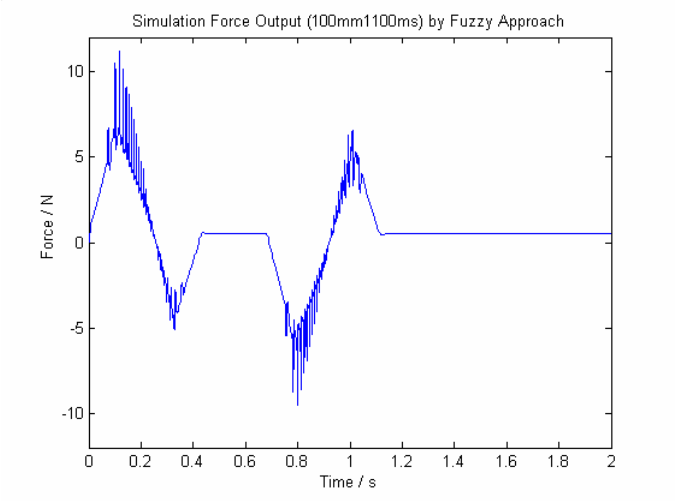

Fig. 5.21: Force output simulated by proposed controller on 100mm.

5.4.2 Short distance (250μm)

For short distance (250μm) simulation, the conventional controller is applied with the maximum dynamic error range 39μm while the proposed controller reduces the error range to be 18μm. Both simulation currents are within 1.4A. The improvement is around 54%. The results are shown in Fig. 5.22-5.27. Similar to the long distance simulation result, the dynamic error, the exciting error and the force are found at the highest acceleration and deceleration.

From the simulation result above, the proposed controller is found to be better on the motion control of LSRM compared with the conventional numerical principle. Different from a typical permanent magnet motor, the LSRM has the nonlinear distribution of magnetic force on the supplied current and at different positions. Since the fuzzy logic control is very robust and need not complicated equations, it is highly recommended to apply it on LSRM motion control.

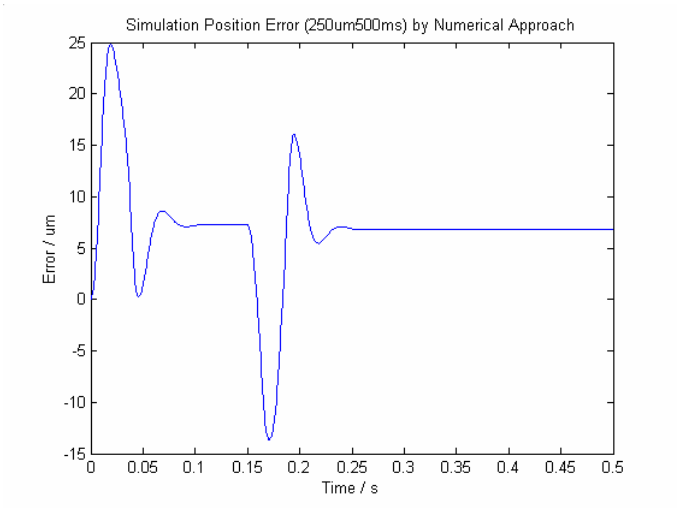

Fig. 5.22: Position error simulated by numerical approach on 250µm.

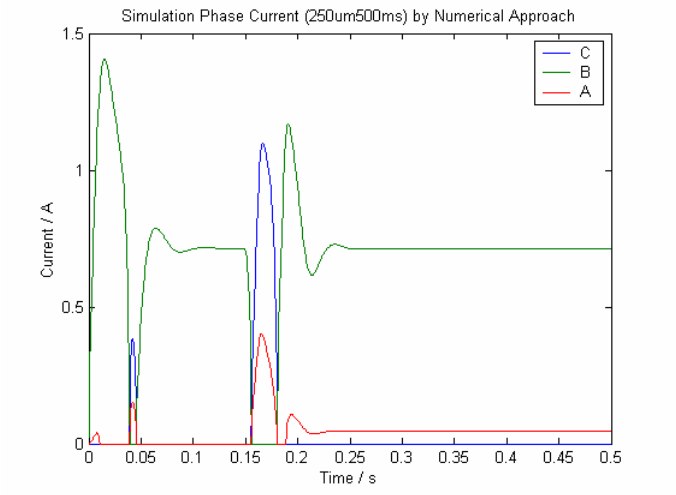

Fig. 5.23: Phase current simulated by numerical approach on 250µm.

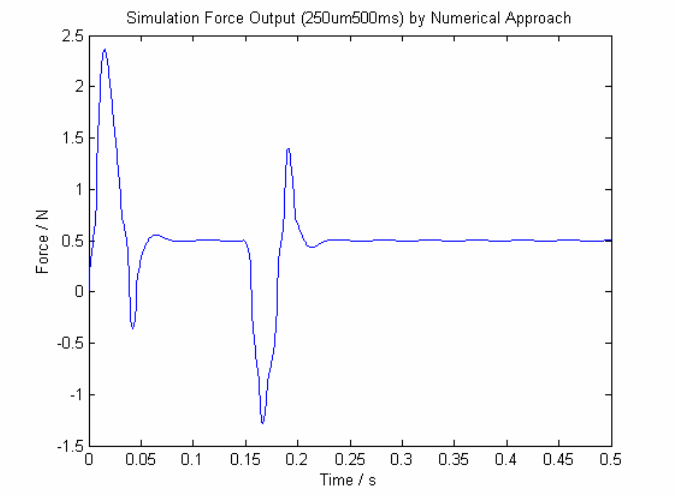

Fig. 5.24: Force output simulated by numerical approach on 250µm.

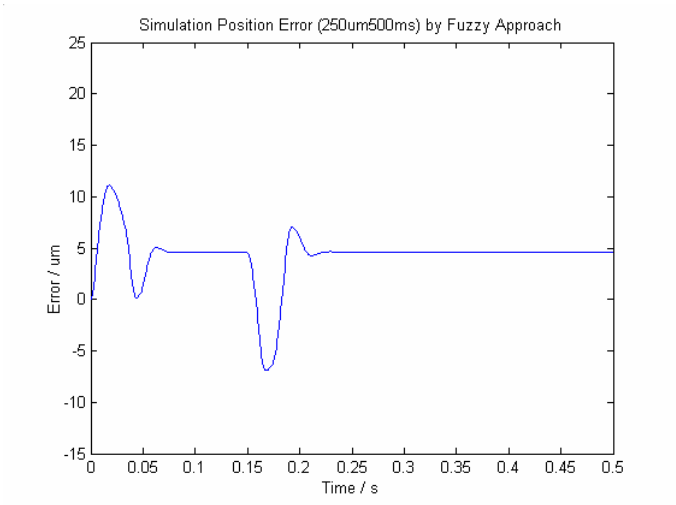

Fig. 5.25: Position error simulated by proposed controller on 250µm.

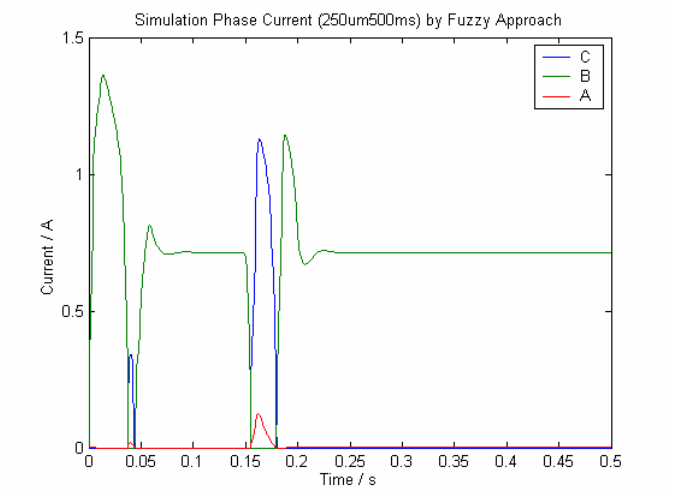

Fig. 5.26: Phase current simulated by proposed controller on 250µm.

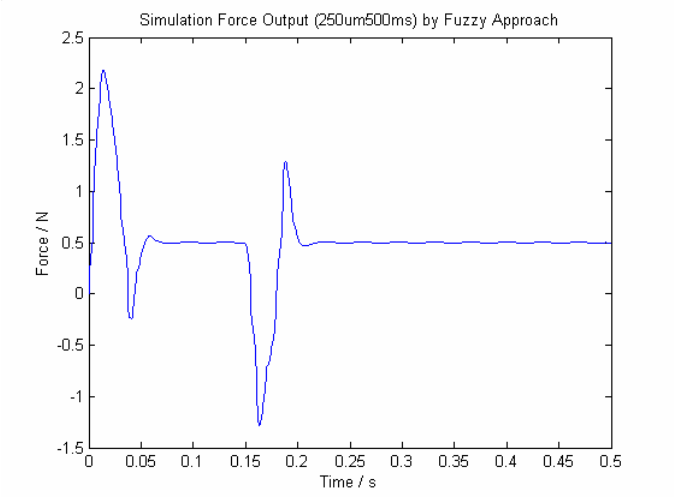

Fig. 5.27: Force output simulated by proposed controller on 250µm.

5.5 Experimental result

In real motor experiments, two traveling distances (100mm & 250μm) are used as the default profiles to compare the performance between conventional and proposed controllers. For each profile, three experiments are taken.

The first test employs the numerical approach as the conventional controller. Based on the simulation result, the proposed fuzzy controller performs better than the conventional numerical controller. To verify the simulation result, the second experiment applies the fuzzy look-up table approach as the proposed controller.

At the outer position control loop, another fuzzy controller is implemented to replace the original PD controller. The motor translator position is measured and compared with the input motion profile to collect the dynamic error. Based on the simulation result, the smaller error range is expected with the higher controller robustness.

5.5.1 Long distance (100mm)

Fig. 5.28 shows the LSRM position response when applying 100mm long distance position profile. The numerical approach contributes the maximum dynamic error 0.4mm. It is only 0.4% of the whole traveling distance. During the whole experiment, all currents applied in the 3 different winding coils are below 3.3A in Fig. 5.29.

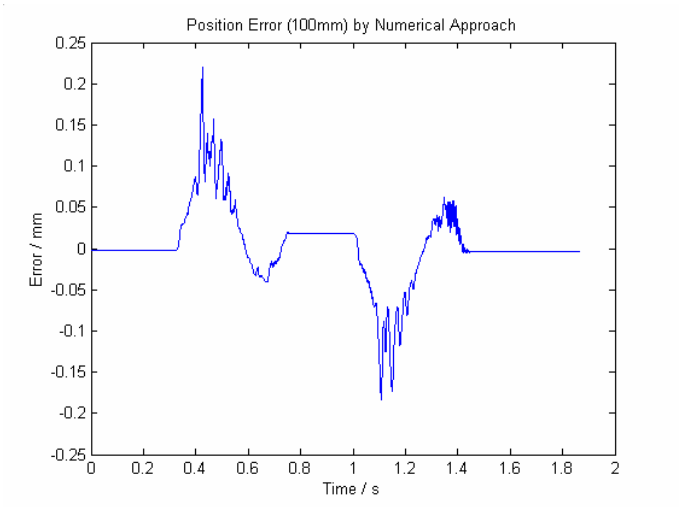

Fig. 5.28: Experimental position error by numerical approach on 100mm traveling.

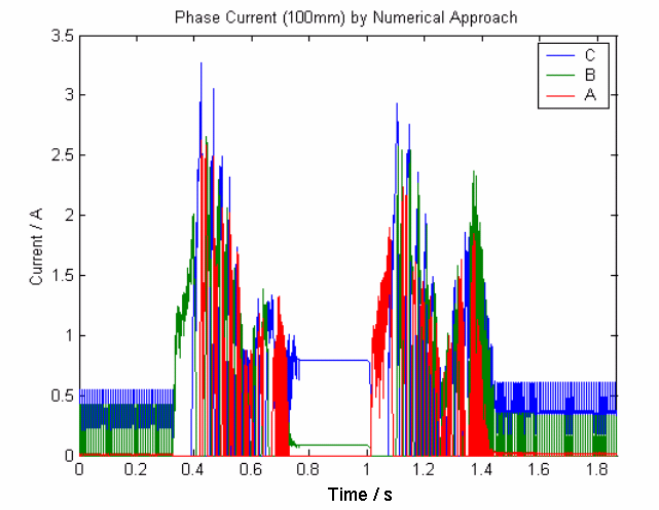

Fig. 5.29: Experimental phase current by numerical approach on 100mm traveling.

Using fuzzy look-up approach, Fig. 5.30 shows that the maximum dynamic error is only 0.35mm and the accuracy is improved significantly by 12.5%. Presented in Fig. 5.31, all three phase currents are still below 3.3A. This implies that the accuracy improvement is not due to the higher peak current but the better allocation of current supplied.

Since the force current distribution in LSRM is different from the typical permanent magnet motor, the special allocation loaded in look-up fuzzification table would solve the problem. Consequently, the controller becomes more intelligent and system can perform more efficiently.

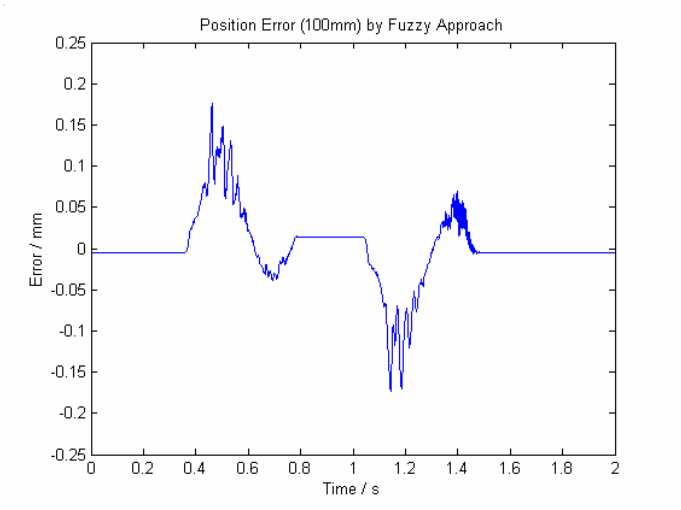

Fig. 5.30: Experimental position error by fuzzy approach on 100mm traveling.

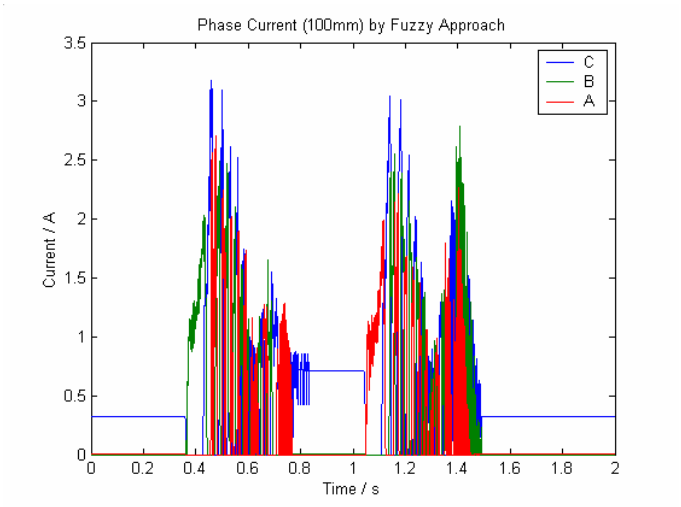

Fig. 5.31: Experimental phase current by fuzzy approach on 100mm traveling.

Beside the use of fuzzy logic in inner control loop, the fuzzification is additionally applied to supervise the position gain and the velocity gain in the outer control loop. Fig. 5.32 shows the maximum dynamic error to be 0.3mm. The accuracy is improved significantly by 14.3%.

Eventually, after implementing two fuzzy controllers in the inner and outer loop, the maximum error is reduced from 0.4mm to 0.3mm with 25% accuracy improvement on 100mm profile. This significant improvement verifies the efficiency of fuzzy logic application in LSRM.

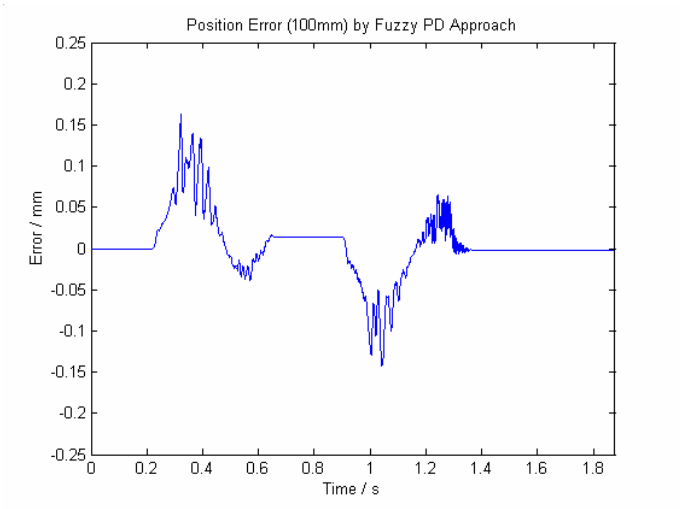

Fig. 5.32: Experimental position error by fuzzy logic supervising PD parameter (100mm).

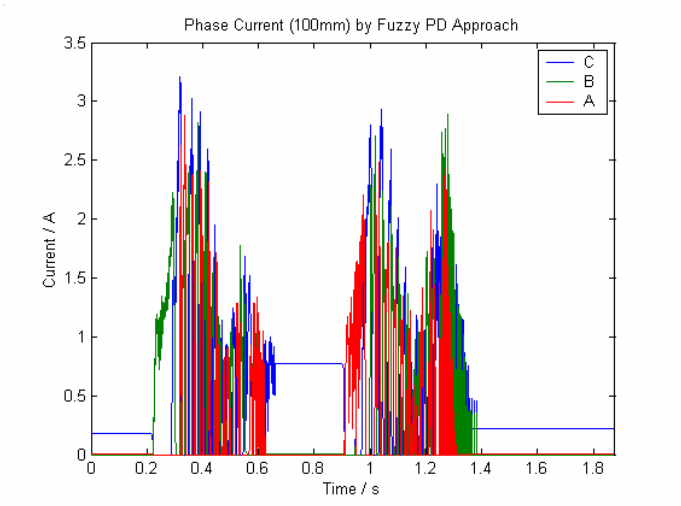

Fig. 5.33: Experimental phase current by fuzzy logic supervising PD parameter (100mm).

5.5.2 Short distance (250µm)

Fig. 5.34 shows the position response when a short distance profile is used. For 250µm profile, the numerical approach runs with maximum dynamic error 46µm and the peak current is 1.3A shown in Fig. 5.35. The maximum error contributes 18.4% of the whole motion profile distance and is much larger than the long distance test result.

Due to very short traveling distance and low current applied in the coils, the static friction and the mechanical sliding guide uncertainty become more significant when compared with the long traveling test.

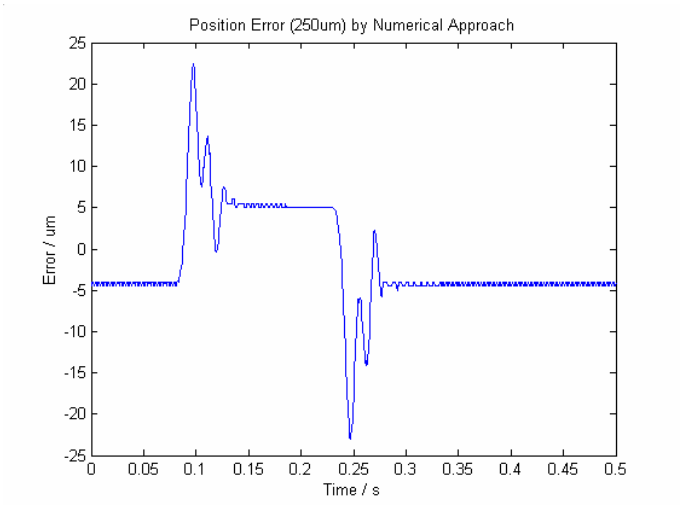

Fig. 5.34: Experimental position error by numerical approach (250µm).

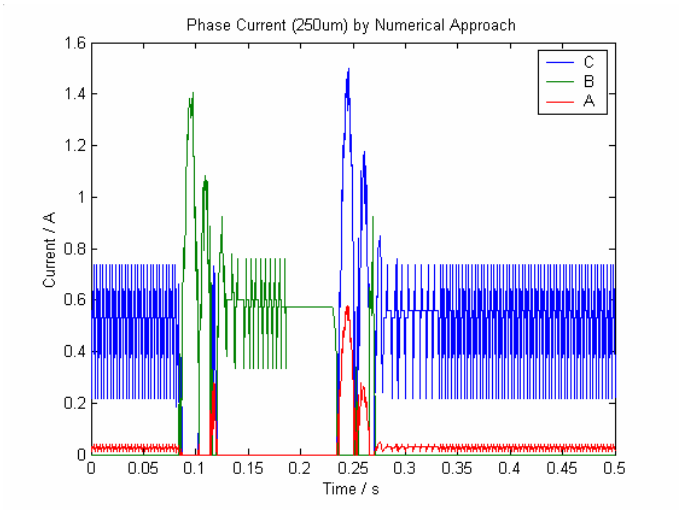

Fig. 5.35: Experimental phase current by numerical approach (250µm).

Using fuzzy look-up approach on force current distribution control, Fig. 5.36 shows the position response. The maximum dynamic error is only 41µm and the accuracy is improved significantly by 11%. Same as the numerical method, all three maximum phase currents are still below 1.3A shown in Fig. 5.37. This implies that the improved performance is not due to the higher current but the smarter allocation of current supplied. Hence, the drive performs in higher efficiency.

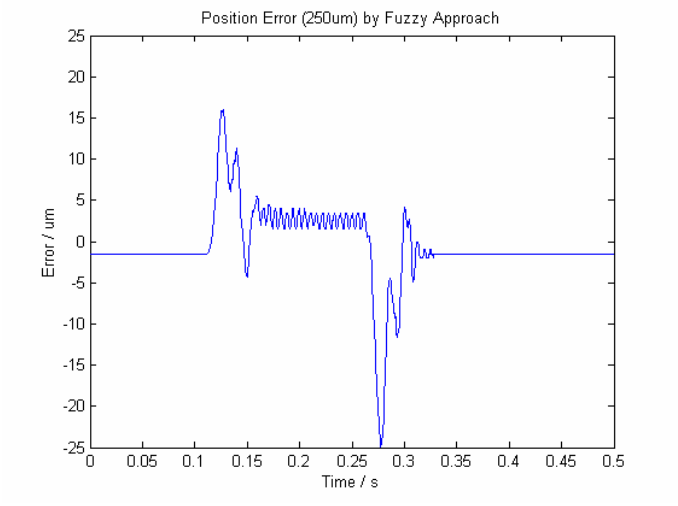

Fig. 5.36: Experimental position error by fuzzy approach (250µm).

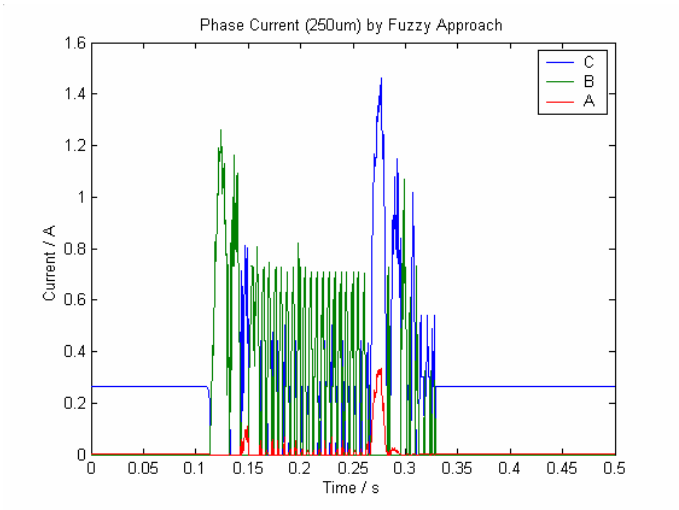

Fig. 5.37: Experimental phase current by fuzzy approach (250µm).

Similar to the long traveling test practice, fuzzy logic algorithm is used in outer position control loop. With the help of fuzzy PD supervising, Fig. 5.38 shows the maximum dynamic error to be 36µm. The accuracy is enhanced largely by 13.9%.

In the consequence, applying the proposed control method, fuzzy logic, in the inner and outer loop for 250µm traveling distance, the maximum error is reduced from 46µm to 36µm. Such 21.7% improvement in motion control accuracy proves that the fuzzy logic controller provides much better performance on LSRM than the conventional numerical approach.

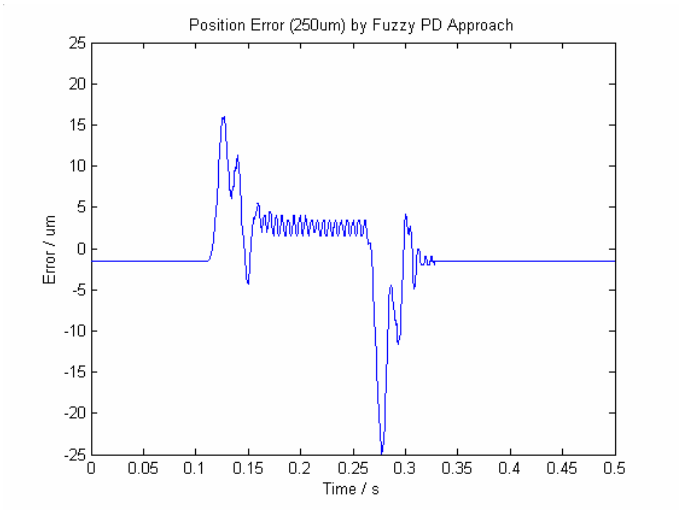

Fig. 5.38: Experimental position error by fuzzy logic supervising PD parameter (250μm).

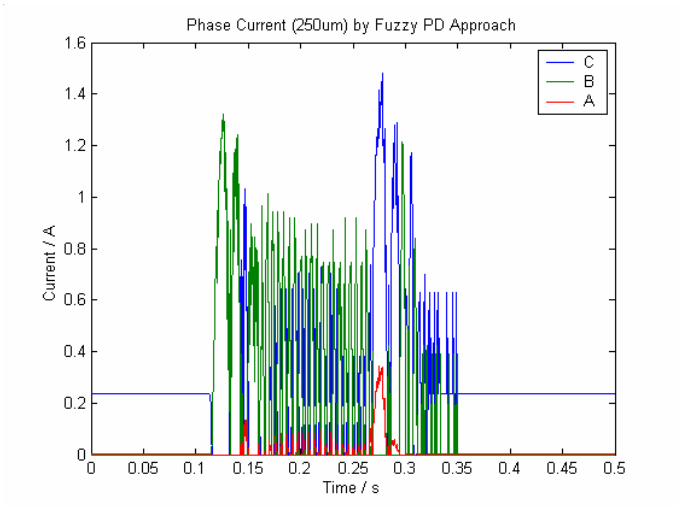

Fig. 5.39: Experimental phase current by fuzzy logic supervising PD parameter (250μm).

Different from the permanent magnet motor, the LSRM has the magnetic flux nonlinear characteristics and cannot be expressed by numerical equations easily. In the conventional controller, the numerical equation expression is usually applied but finds difficulties. In order to solve this problem, the look-up table fuzzification is proposed since it can well present such nonlinear characteristic in

LSRM inner control loop.

From the above experiments taken for long distance (100mm) and short distance (250μm), the LSRM position error is compared between numerical and fuzzy logic controller. The significant improvement in two extreme traveling distance tests proves the argument above.

There are some discrepancies between the experimental result and the simulation result. In simulation, the dynamic error is reduced by almost 50% after applying fuzzy approach. In experiment, the dynamic error is improved by 10% only because of mechanical uncertainty and magnetic field inconsistency. To simplify the simulation, it is assumed that no magnetic field leakage occurs and the frictional force between the moving platform and the track remained unchanged.

The PD feedback controller is commonly used in control industry. However, the PD parameters have to be finely tuned for different traveling distances. In addition, this fine tuning procedure requires the knowledge and experience of control experts. Fuzzy PD supervising ability is very useful to save these experts manpower and allow general operators to handle some nonlinear system.

For the LSRM outer control loop, the PD fuzzy supervising is proposed. In two different motion profile tests, the experimental result highlights the advantages of fuzzy logic control and proves its efficiency.

5.6 Summary of position accuracy improvement

5.6.1 Long distance (100mm)

Table 5.1: Position accuracy summary of long distance (100mm) traveling.

Motor control scheme	**Max. error range**	**Improvement**	**Comparison**
Numerical approach (A)	0.4mm	N/A	N/A
Table look-up fuzzification (B)	0.35mm	12.5%	Fig. 5.40
Table look-up fuzzification + PD supervision (C)	0.3mm	25%	Fig. 5.41

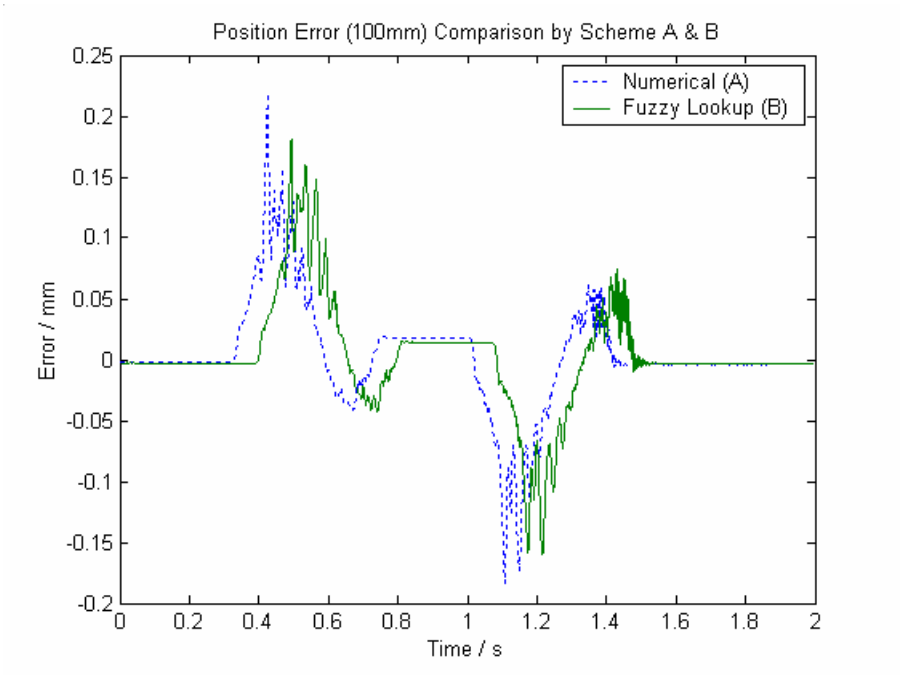

Fig. 5.40: Experimental position error by numerical and fuzzy approach on 100mm traveling.

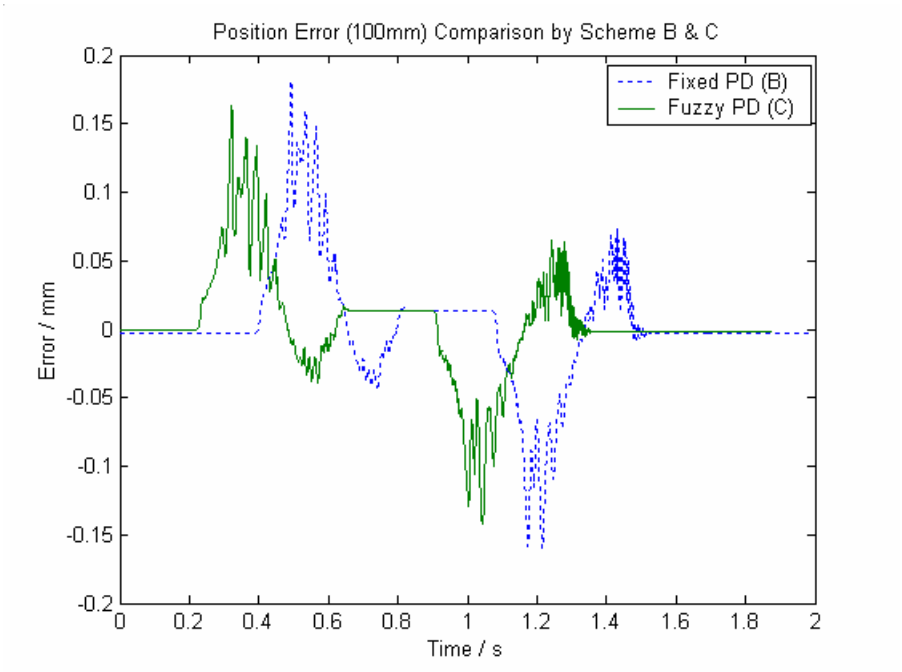

Fig. 5.41: Experimental position error by fixed PD and fuzzy logic supervising PD parameter approach on 100mm traveling.

5.6.2 Short distance (250µm)

Table 5.2: Position accuracy summary of short distance (250µm) traveling.

Motor control scheme	**Max. error range**	**Improvement**	**Comparison**
Numerical approach (A)	46µm	N/A	N/A
Table look-up fuzzification (B)	41µm	11%	Fig. 5.42
Table look-up fuzzification + PD supervision (C)	36µm	21.7%	Fig. 5.43

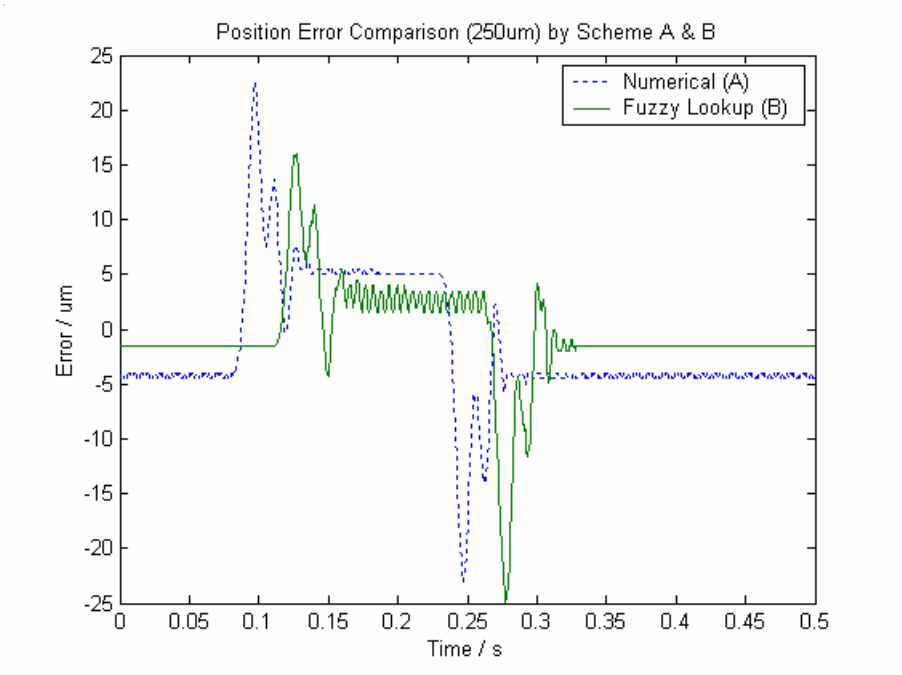

Fig. 5.42: Experimental position error by numerical and fuzzy approach on 250μm traveling.

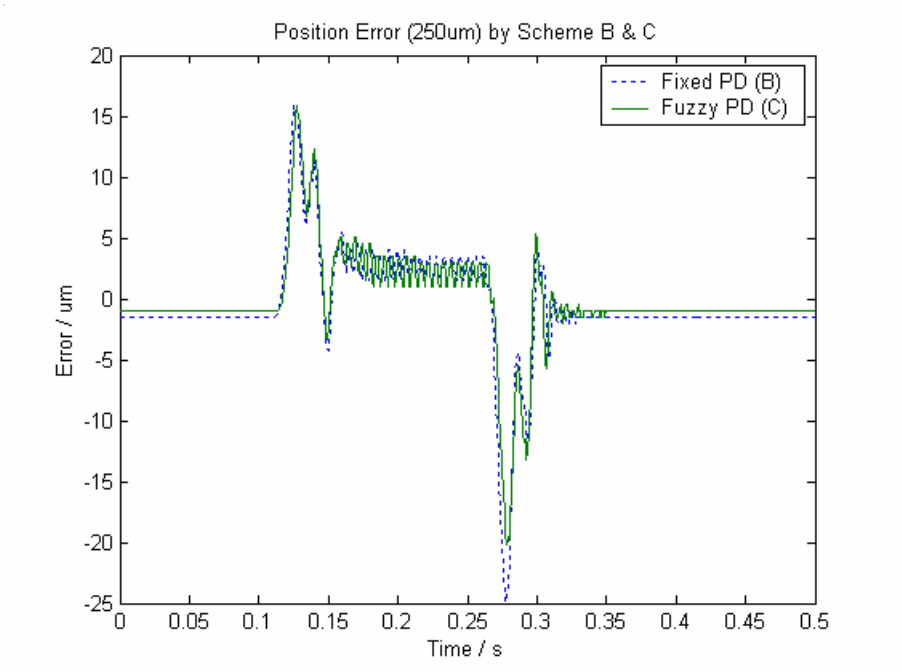

Fig. 5.43: Experimental position error by fixed PD and fuzzy logic supervising PD parameter approach on 250μm traveling.

Chapter 6

Conclusions and further research

Based on the effort of the LSRM project, the improvement on the motor and the research work on the controller are concluded. After that, another research area is suggested to further improve the LSRM system.

6.1 Conclusions

In this research project, a robust LSRM system with an advanced mechanical structure and a reliable controller is developed.

From the view of mechanical structure, three different types of LSRM are discussed. On the finalized prototype, the model rigidity is further improved with advanced assembly method. Additional machining procedure is suggested to guarantee the constant air gap between the translator and stator and improve the motor productivity. Therefore, the LSRM prototype is capable to achieve high speed motion precisely.

Applying switched reluctance technology, the conventional numerical controller always faces motion control problem due to magnetic flux nonlinearity. Proven by simulation and experimental result on different traveling distances, the proposed fuzzificed current force representation scheme is successful to provide an accurate and high efficiency controller on LSRM.

Beside the inner control loop regarding to exciting current and magnetic force, another fuzzy logic system supervising PD controller is proposed to reserve manpower on motion tuning. The significant position accuracy improvement shows the extremely high robustness of the applied fuzzy controller.

Combining the experimental results on inner control loop with current force

relationship and outer control loop on PD parameter supervision, the fuzzy logic improves motor performance at least 20%. With the successful application of the fuzzy logic on LSRM position control, the LSRM in this project is very robust and capable to have a high precision motion performance. Based on the LSRM characteristics of simple structure, high flexibility under different temperature and economic manufacturing, it is a potential candidate to alternate linear three-phase PM/induction motors in special applications that require the features of magnet-free and high temperature operation. With the proposed controllers, LSRM is definitely becoming popular in precision machine industry.

6.2 Further research

To further improve the LSRM performance and robustness, it is suggested to explore a sensorless control technique to replace the existing optical encoder. With this additional information for motion feedback control, the whole LSRM needs not to install any electronics device. As a result, the LSRM can operate at extremely wide range of temperature and be implemented with reduced equipment cost.

Appendix

List of publications arising from the project

Journal Paper

[1] S. C. Kwok, W. C. Gan, N. C. Cheung and S. L. Ho, “Applications of fuzzy logic control to linear switched reluctance motors”. *Electric Power Components and Systems, 2008 - submitted for published*, April., 2008.

[2] W. C. Gan, N. C. Cheung and A. S. C. Kwok, “A Novel Solar Tracking System Design Based on Linear Switched Reluctance Motor”, *2007 Journal of Control Theory and Applications*, vol. 25, no. 2, April 2008

Conference Proceedings

[1] A. S. C. Kwok, W. C. Gan and N. C. Cheung, “Improvements in the motion accuracy of linear switched reluctance motors”. *2008 IEEE World Congress on Computational Intelligence, ,* Hong Kong, 1-6 June, 2008.

[2] S. C. Kwok, W. C. Gan and N. C. Cheung, “Improvements in the mechanical structure of the linear switched reluctance motor’, *2006 2nd International Conference on Power Electronics System and Applications*, pp.186-189, Nov., 2006.

[3] J. F. Pan, N. C. Cheung, S. C. Kwok and J. Yang, “Auto disturbance rejection speed control of linear switched reluctance motor”, *IAS Annual Meeting. Conference Record of the 2005*, vol. 4, pp.2491-2497, Oct., 2005.

References

[1] T. J. E. Miller, *Switched Reluctance Motor and Their Control*, Magna Physics Publishing and Clarendon Press, Oxford, 1993.

[2] R. Krishnan, *Switched Reluctance Motor Drives: Modeling, Simulation, Analysis, Design, and Applications*, C.R.C. Press, 2001.

[3] R. C. Dorf and R. H. Bishop, *Modern Control Systems*, Addison Wesley, 1998.

[4] I. S. Shaw, *Fuzzy Control of Industrial Systems: Theory and Applications*, Kluwer Academic Publishers, 1998.

[5] L. X. Wang, *Adaptive Fuzzy Systems and Control: Design and Stability Analysis*, Prentice Hall PTR, 1994.

[6] B. S. Lee, H. K. Bae, P. Vijayraghavan and R. Krishnan, "Design of a linear switched reluctance machine," *IEEE Transactions on Industry Applications*, vol. 36, no. 6, pp.1571-1580, Nov., 2000.

[7] N. Matsui, N. Akao and T. Wakino, "High-precision torque control of reluctance motors", *IEEE Transactions on Industry Applications*, vol.27, no.5, Sep/Oct., 1991.

[8] S. C. P. Gomes and J. P. Chretien, "Dynamic modelling and friction compensated control of a robot manipulator joint," *IEEE International Conference on Robotics and Automation*, vol. 2, pp. 1429-1435, May, 1992.

[9] M. G.. Rodrigues, W. I. Suemitsu, P. Branco, J. A. Dente and L. G. B. Rolim, "Fuzzy logic control of a switched reluctance motor", *Proceedings of the IEEE International Symposium on Industrial Electronics*, vol. 2, pp. 527-531, Jul., 1997.

[10] A. E. Santo, M. R. A. Calado and C. M. P. Cabrita, "Long stroke linear switched reluctance actuator displacement with a fuzzy logic controller", *IEEE MELECON 2006*, pp. 1178-1181, May, 2006.

[11] H. Chen, J. Jiang, S. Sun and D. Zhang, "Dynamic simulation models of switched reluctance motor drivers", *IEEE Proceedings of the 3rd World Congress on Intelligent Control and Automation*, vol. 3, pp. 2111-2115, Jul., 2000.

[12] I. Husain, "Minimization of torque ripple in SRM drives", *IEEE Transactions on Industrial Electronics*, vol. 49, no. 1, pp. 28-39, Feb., 2002.

[13] L. X. Wang, *A Course in Fuzzy Systems and Control*, Prentice Hall PTR, 1997.

[14] H. Ying, *Fuzzy Control and Modeling: Analytical Foundations and Applications*, IEEE Press, 2000.

[15] N.C. Cheung, "A robust and low-cost linear motion system for precision manufacturing automation", *IEEE Industry Applications Conference*, vol. 1, pp. 40-45, Oct., 2000.

[16] N.C. Cheung, "A new type of direct-drive variable reluctance actuators for industrial automation", *IEEE International Conference on Industrial Technology*, vol. 1, pp. 30-34, 2002.

[17] W. C. Gan and N.C. Cheung, "Development and control of a low-cost linear variable-reluctance motor for precision manufacturing automation", *IEEE/ASME Transactions on Mechatronics*, vol. 8, no. 3, pp. 326-333, Sep., 2003.

[18] W.C. Gan, N.C. Cheung and L. Qiu, "Position control of linear switched reluctance motors for high-precision applications", *IEEE Transactions on Industry Applications*, vol. 39, no. 5, Sep., 2003.

[19] W.C. Gan, N.C. Cheung, "Design of a linear switched reluctance motor for high precision applications", *IEEE International Electric Machines and Drives Conference*, pp. 701-704, Jun., 2001.

[20] W.C. Gan, N.C. Cheung and L. Qiu, "Short distance position control for linear switched reluctance motors: a plug-in robust compensator approach", *Conference Record of the 2001 IEEE Industry Applications Conference. 36th IAS Annual Meeting*, vol. 4, pp. 2329-2336, Oct., 2001.

[21] D. Dolinar, G. Stumberger and M. Milanovie, "Tracking improvement of LSRM at low-speed operation", *European Transactions on Electrical Power*, vol. 15, pp.257-270, 2005.

[22] Y. Liu and P. Pillay, "Improved torque performance of switched reluctance machines by reducing the mutual saturation effect", *IEEE Transactions on Energy Conversion*, vol. 19, no. 2, Jun., 2004.

[23] F. M. El-khouly, "High performance direct torque control of switched reluctance motor drives", *Electric Power Components and Systems*, vol. 33, pp. 287-297, 2005.

[24] G. G. Lopez, P. C. Kjaer and T. J. E. Miller, "High-grade position estimation for SRM drives using flux linkage / current correction model", *IEEE Transactions on Industry Applications*, vol. 35, no. 4, Jul., 1999.

[25] A. Tenhunen, T. P. Holopainen and A. Arkkio, "Effect of saturation on the forces in induction motors with whirling cage motor", *Proceedings of Compumag*, vol. II, pp. 66-67, Jul. 2003.

[26] Y. X. Su, B. Y. Duan and Y. F. Zhang, "Robust precision motion control for AC

servo system", *Proceedings of the 4th World Congress on Intelligent Control and Automation*, pp. 3319-3323, Jun., 2002.

[27] L. O. A. P. Henriques, P. J. C. Branco, L. G. B. Rolim and W. I. Suemitsu, "Proposition of an offline learning current modulation for torque-ripple reduction in switched reluctance motors: design and experimental evaluation", *IEEE Transactions on Industrial Electronics*, vol. 49, no. 3, pp. 1-13, 2002.

[28] P. C. Kjacer, J. J. Gribble and T. J. E. Miller, "High-grade control of switched reluctance machines", *IEEE Transactions on Industry Applications*, vol. 33, no. 6, Nov/Dec., 1997.

[29] U. S. Deshpande, J. J. Cathey and E. Richter, "High-force density linear switched reluctance machine", *IEEE Transactions on Industry Applications*, vol. 31, no. 2, Mar/Apr., 1995.

[30] H. K. Bae, B. S. Lee, P. Vijayraghavan and R. Krishnan, "A linear switched reluctance motor: converter and control", *IEEE Transactions on Industry Applications*, vol. 36, no. 5, Sep/Oct., 2000.

[31] N. Inang, A. Derdiyak and V. Ozbulur, "Fuzzy logic control of a switched reluctance motor including mutual inductances and operating in the linear region", *Proceedings of the 12th IEEE International Symposium on Intelligent Control*, Jul., 1997.

[32] H. Chen, D. Zhang, Z. Y. Cong and Z. F. Zhang, "Fuzzy logic control for switched reluctance motor drive", *Proceedings of the First International Conference on Machine Learning and Cybermetics*, pp. 145-149, Nov., 2002.

[33] A. D. Cheok and N. Ertugrul, "Use of fuzzy logic for modeling, estimation, and prediction in switched reluctance motor drives", *IEEE Transactions on Power Electronics*, vol. 46, no. 6, pp. 1207-1224, Dec., 1999.

[34] N. Ertugrul and A. D. Cheok, "Indirect angle estimation in switched reluctance

motor drives using fuzzy logic based motor model", *IEEE Transactions on Power Electronics*, vol. 15, no. 6, pp. 1029-1044, Nov., 2000.

[35] A. D. Cheok and N. Ertugrul, "High robustness and reliability of fuzzy logic based position estimation for sensorless switched reluctance motor drives", *IEEE Transactions on Power Electronics*, vol. 15, no. 2, pp. 319-334, Mar., 2000.

[36] A. Tzes, P. Y. Peng and J. Guthy, "Genetic-based fuzzy clustering for DC-motor friction identification and compensation", *IEEE Transactions on Control Systems Technology*, vol. 6, no. 4, pp. 462-472, Jul., 1998.

[37] F. L. Lewis, W. K. Tim, L. Z. Wang and Z. X. Li, "Deadzone compensation in motion control systems using adaptive fuzzy logic control", *IEEE Transactions on Control Systems Technology*, vol. 7, no. 6, pp. 731-742, Nov., 1999.

[38] J. T. Teeter, M. Y. Chow and J. J. Brickley, "A novel fuzzy frication compensation approach to improve the performance of a dc motor control system", *IEEE Transactions on Industrial Electronics*, vol. 43, no. 1, pp. 113-120, 1996.

[39] G. S. Buja and M. I. Valla, "Control characteristics of the srm drives. Part I: operation in the linear region", *IEEE Transactions on Industrial Electronics*, vol. 38, no. 5, pp. 313-321, 1991.

[40] G. S. Buja and M. I. Valla, "Control characteristics of the srm drives. Part II: operation in the saturated region", *IEEE Transactions on Industrial Electronics*, vol. 41, no. 3, pp. 316-325, 1994.

[41] S. Bolognani and M. Zigliotto, "Fuzzy logic control of a switched reluctance motor drive", *IEEE Transactions on Industry Applications*, vol. 32, no. 5, Sep/Oct., 1996.